

Flexible Electronics

International Edition: DOI: 10.1002/anie.201809781

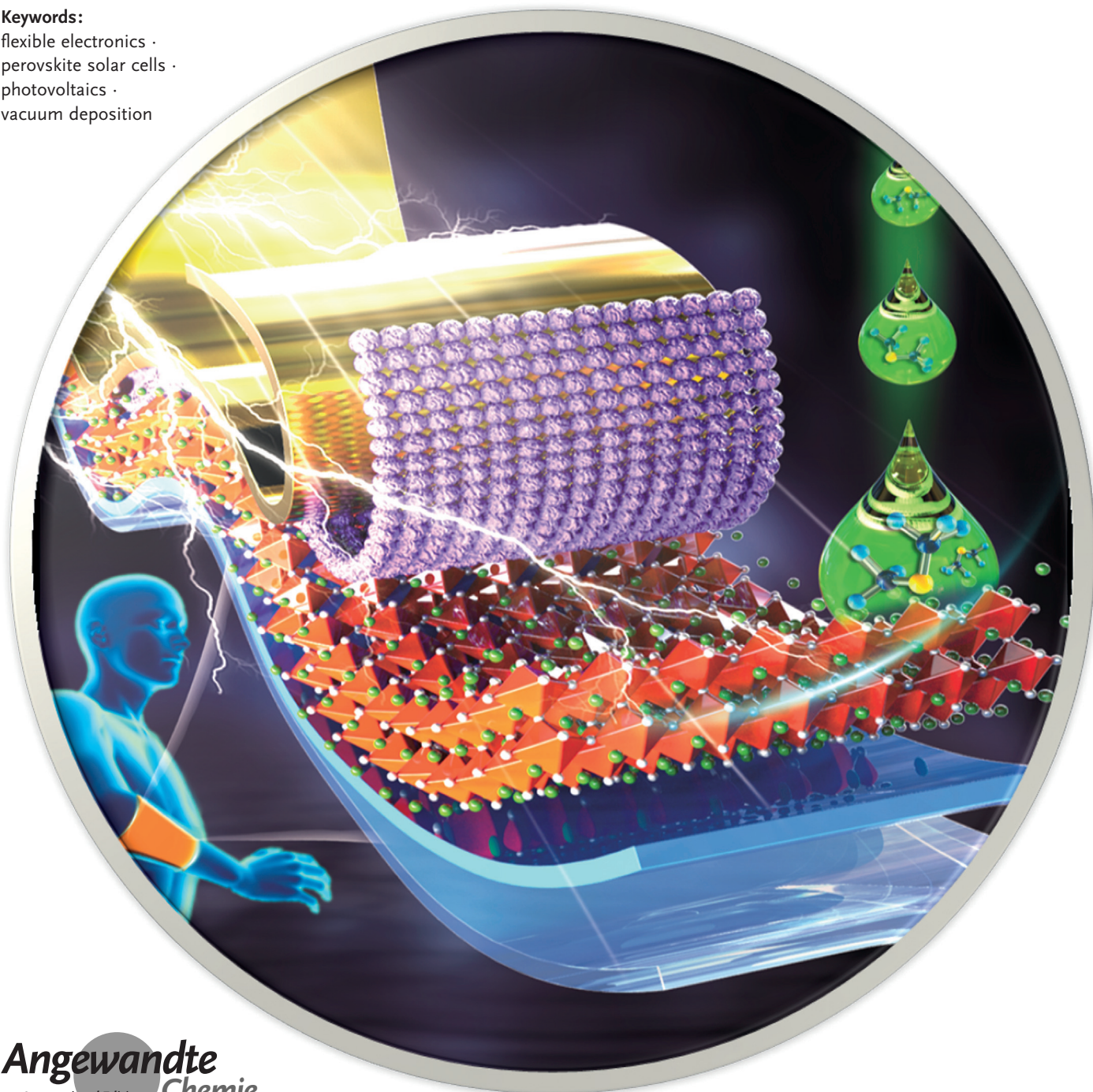
German Edition: DOI: 10.1002/ange.201809781

Recent Advances in Flexible Perovskite Solar Cells: Fabrication and Applications

Dong Yang⁺, Ruixia Yang⁺, Shashank Priya,^{*} and Shengzhong (Frank) Liu^{*}

Keywords:

flexible electronics ·
perovskite solar cells ·
photovoltaics ·
vacuum deposition



Flexible perovskite solar cells have attracted widespread research effort because of their potential in portable electronics. The efficiency has exceeded 18% owing to the high-quality perovskite film achieved by various low-temperature fabrication methods and matching of the interface and electrode materials. This Review focuses on recent progress in flexible perovskite solar cells concerning low-temperature fabrication methods to improve the properties of perovskite films, such as full coverage, uniform morphology, and good crystallinity; demonstrated interface layers used in flexible perovskite solar cells, considering key figures-of-merit such as high transmittance, high carrier mobility, suitable band gap, and easy fabrication via low-temperature methods; flexible transparent electrode materials developed to enhance the mechanical stability of the devices; mechanical and long-term environmental stability; an outlook of flexible perovskite solar cells in portable electronic devices; and perspectives of commercialization for flexible perovskite solar cells based on cost.

1. Introduction

Solar power is considered the most important renewable energy resource because it is clean, inexhaustible, import-independent, and affordable. The advanced use of the solar energy does not cause further pollution or damage to our environment like traditional fossil fuels.^[1] In recent decades, various technologies have been developed to harness the solar energy, such as solar heating,^[2] solar architecture,^[3] photovoltaics,^[4] artificial photosynthesis,^[5] photocatalytic water splitting.^[6,7] Among these, photovoltaics that convert sunlight into electricity has attracted comprehensive attention because it is capable of providing sufficient amount of energy to satisfy all our power demands without causing any pollution to our environment for foreseeable future of humankind. Thus far, various types of solar cells have been developed, for example, polycrystalline silicon solar cells (mc-Si cells),^[8] single-crystalline silicon solar cells (c-Si cells),^[9–11] thin film silicon solar cells,^[12,13] CdTe based solar cells,^[14,15] CIGS solar cells,^[16,17] GaAs based solar cells,^[18] CZTS,^[19–21] dye-sensitized solar cells (DSSCs),^[22] quantum dot-sensitized solar cells (QDSSCs),^[23] organic photovoltaics (OPVs),^[24] and perovskite solar cells (PSCs).^[25] For solar cells, the most important figures-of-merit for commercialization are power on version efficiency (PCE) and cost. At the present stage, the long-term stability and toxicity are also important issues for perovskite-based photovoltaic technology.

With the rapid development of advanced technologies in the electronics industry, the demand for portable electronics, shaped display devices and wearable electronic textiles is ever-increasing. Flexible solar cells are therefore receiving more and more attention for their favorable traits, including flexibility, light weight, portability, and compatibility with curved surfaces.^[11] More importantly, mass production of the flexible solar cells can be achieved by continuous roll-to-roll technology. This is a huge advantage in comparison with the batch-to-batch operation for rigid cells that is associated with

reduced manufacture speed, more complicated equipment, and higher cost. Furthermore, the rigid solar cells are much heavier and thicker, they are therefore more costly for storage and transportation. On the other hand, flexible solar cells are lighter in weight, thinner, and more bendable for storage, transportation, and installation, which greatly reduce all related costs, especially when they are often installed in remote areas, such as islands, mountains, and deserts.^[26] Their advantages are even more outstanding when they are used in flights and for stratosphere and space applications. Therefore, research on developing high-efficiency flexible solar cells is of

From the Contents


1. Introduction	4467
2. Low-Temperature Flexible Perovskite Films	4469
3. Low-Temperature Interface Layers	4472
4. Flexible Electrodes	4474
5. Stability of Flexible Perovskite Photovoltaics	4475
6. Flexible Perovskite Photovoltaics Applied in Portable Electronic Devices	4478
7. Potential Commercialization	4478
8. Conclusion and Outlook	4479


[*] Dr. D. Yang,^[+] R. Yang,^[+] Prof. S. Liu
Key Laboratory of Applied Surface and Colloid Chemistry, Ministry of Education; Shaanxi Engineering Lab for Advanced Energy Technology, School of Materials Science and Engineering, Shaanxi Normal University, 620 West Chang'an Avenue, Xi'an 710119 (China)

Prof. S. Liu
Dalian National Laboratory for Clean Energy, iChEM
Dalian Institute of Chemical Physics, Chinese Academy of Sciences
457 Zhongshan Road, Dalian 116023 (China)
E-mail: szliu@dicp.ac.cn

Dr. D. Yang,^[+] Prof. S. Priya
Materials Science and Engineering, Penn State
University Park, PA 16802 (USA)
E-mail: spriya@vt.edu

[*] These authors contributed equally to this work.

 The ORCID identification number(s) for the author(s) of this article can be found under:
<https://doi.org/10.1002/anie.201809781>.

 © 2018 The Authors. Published by Wiley-VCH Verlag GmbH & Co. KGaA. This is an open access article under the terms of the Creative Commons Attribution Non-Commercial License, which permits use, distribution and reproduction in any medium, provided the original work is properly cited, and is not used for commercial purposes.

great significance. Thus far, crystalline silicon solar cells, owing to their high efficiency, have dominated solar cell markets, with a circa 90% market share.^[8] However, the rigid configuration, high manufacturing costs, and heavy weight make the crystalline silicon solar cells not only unsuitable to roll-to-roll continuous mass production, but also incompatible with the flexible electronics design.^[27] In these regards, the multijunction thin-film silicon solar cell has been recognized as a celebrity; unfortunately it suffers from its complicated fabrication processes associated with expensive equipment cost and low efficiency, limiting its use to only special niche applications.^[28] Even though there have been a range of thin film solar cells developed, such as DSSCs, QDSSCs, and OPVs, with even lower efficiency and inferior stability, they are still too primitive for commercial applications.^[27,29,30]

Organic–inorganic halide perovskite, with the characteristic chemical formula ABX_3 , was first demonstrated by Mitzi and co-workers to be applied in light-emitting diodes and transistors in the 1990s,^[31,32] where A typically uses methylammonium (MA^+ , $CH_3NH_3^+$) or formamidinium (FA^+ , $CH_3CH_2NH_3^+$), B divalent metal ions such as Pb^{2+} or Sn^{2+} , and the X halide anions (I^- , Br^- , Cl^-) binding to both cations A and B. In 2009, Miyasaka and co-workers reported the initial application of perovskite materials in solar cells,^[33] in which $CH_3NH_3PbX_3$ (X: I, Br) was used as the sensitizer in a typical liquid-electrolyte-based DSSC structure. Although the efficiency obtained was only 3.81%, they introduced a brand-new photovoltaic material. Subsequent studies revealed more advantages of the perovskite material, including amazing tolerance to defects, tunable band gaps, high absorption coefficients, small exciton binding energies, long charge diffusion lengths, high carrier mobilities, ultra-low trap densities, and so on,^[34–37] making the organic–inorganic PSCs extremely appealing candidates for photovoltaic applications.

Moreover, owing to the accessibility and abundance of the precursor components for the perovskites as well as ease of fabrication using a range of thin film deposition techniques including atmospheric solution processing^[38,39] and vacuum deposition,^[40,41] a list of remarkable breakthroughs have been attained within a short period of time, with the PCE rapidly increased to as high as 23.3%,^[42] making it the highest efficiency among all thin film solar cells measured under normal sunlight intensity.^[8] Apart from its high efficiency, all its precursor materials are abundant on earth and all fabrication procedures can be completed at temperature below 150°C, making it ideal for high efficiency flexible solar cells. Strong optical absorption across the visible spectrum is a key figure-of-merit required for high-performance active absorber layer material. The perovskite thin films have demonstrated excellent absorption in this regard, only about 300 nm thick film is sufficient to absorb essentially all visible light above its band gap.^[43] Furthermore, its absorption range or band gap can be adjusted by varying the components in the perovskite structure. For example, the substitution of FA for MA in the triiodide perovskites extends the absorption range from about 780 nm to about 830 nm.^[44] The absorption edge can be continuously tuned from 786 nm to 544 nm by increasing the Br content in the I/Br mixed MA-based perovskites.^[45] Moreover, mixed Sn/Pb triiodide perovskite broadens the absorption spectrum to beyond 1100 nm.^[38] Note that these results show that the band gap of the perovskites can be tuned via simple element mixing process,^[46] making it possible to design matched carrier transport layers for enhanced device performance. On the other hand, because the commonly used polymer substrate for flexible solar cells cannot withstand high temperature beyond 250°C, all deposition and treatment processes have to be conducted at significantly lower temperature to ensure that the substrate



Dong Yang received his PhD degree in physical chemistry from Dalian Institute of Chemical Physics, Chinese Academy of Sciences in 2014. After graduation, he worked as a post-doctoral fellow in Shaanxi Normal University (2014–2017), Virginia Tech (2017–2018). Currently, he is an assistant research professor in Penn State University, and he is also a professor in Shaanxi Normal University. His research fields focus on semiconductors and organic and perovskite solar cells.



Shashank Priya is currently a professor in department of materials science and engineering at Penn State University. He is also adjunct Professor in department of mechanical engineering in Virginia Tech. His research areas are energy harvesting, multifunctional materials, and bioinspired robotics. He is founder and chair of Annual Energy Harvesting Workshop series and Annual Energy Harvesting Society Meeting. Dr. Priya is a member of the Honorary Chair Committee for the International Workshop on Piezoelectric Materials and Applications.



Ruixia Yang received her master's degree in organic chemistry from Dalian University of Technology in 2011 and worked as an assistant professor in Dalian Institute of Chemical Physics, Chinese Academy of Sciences, from 2011 to 2017. Her research field was the synthesis of materials for photovoltaic devices and organic light-emitting diodes (OLEDs).



Shengzhong (Frank) Liu received his Ph.D. from Northwestern University (USA) in 1992. Following his postdoctoral research at Argonne National Laboratory (Argonne, Illinois, USA), he worked for various companies researching nanoscale materials, thin film solar cells, laser processing, and diamond thin films. His invention of the semi-transparent photovoltaic module at BP Solar won an R&D 100 award in 2002. He is now a professor at Shaanxi Normal University and Dalian Institute of Chemical Physics, Chinese Academy of Sciences.

would not be negatively affected. In the last few years, various low-temperature methods have been developed to fabricate perovskite films, such as one-step solution deposition, two-step sequential solution deposition, solvent-quenching, dual source vacuum co-evaporation, alternating precursor deposition, solid source direct contact fabrication, and so on.^[47] Many studies have demonstrated that high-quality perovskite thin films with uniform morphology, full surface coverage, free of pin-holes, and good crystallinity can be successfully prepared using these methods at relatively low temperature, implying that these processes are promising candidate for the perovskite layer fabrication on flexible substrate. Furthermore, it has been reported that solution-processed organo-lead trihalide perovskites show high charge-carrier mobilities, which is conducive to high-performance flexible solar cells.^[48] Recently, researchers have focused more their attention on designing low-cost, lightweight, and mechanically flexible PSCs. Figure 1 shows the development milestone for flexible PSCs. It is clear that since the first report of flexible PSCs with PCE of 2.62% by Mathews' group in 2013,^[49] the efficiency has been rapidly closed to 18.4%.^[50,51] These works enable the implementation of portable, large-area and even roll-to-roll fabrication of PSCs at low temperature, which can potentially contribute to dramatically lowering the production costs of flexible perovskite modules.

In the following sections, we review the recent progress on flexible PSCs based on different functional layers fabricated

by low-temperature fabrication technologies, and discuss the mechanical and long-term environmental stability for flexible PSCs. Then we prospect the flexible PSCs in portable electronic device, and estimate the cost of flexible PSCs prepared by roll-to-roll vacuum deposition technology. Furthermore, the prospective and further developments of flexible PSCs will be suggested and discussed.

2. Low-Temperature Flexible Perovskite Films

Since the appearance of PSCs, great efforts have been made to obtain high-quality perovskite thin films with full coverage, lack of pin-holes, and high crystallinity, especially using simple and low-cost fabrication methods. In this section, we discuss the different technologies used to fabricate perovskite films at low temperature.

2.1. One-Step Deposition

In the one-step deposition method, the mixed precursor solution, containing MA/FA halides and metal halides with a stoichiometric (1:1) or non-stoichiometric (3:1) molar ratio, is directly deposited onto the desired substrates by a one-step spin-coating procedure. The samples are then annealed at low temperature (100 °C) to yield perovskite films.^[52] Yang's

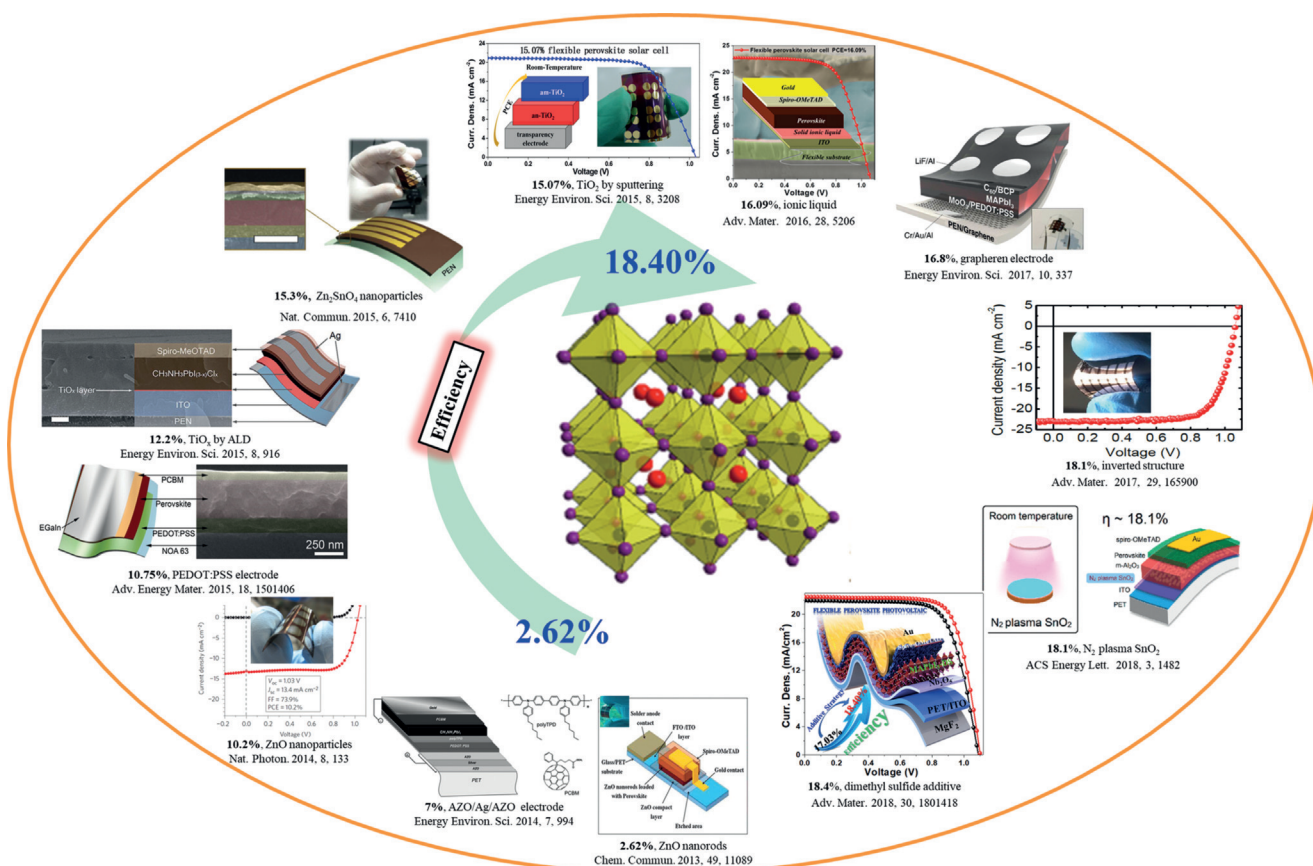


Figure 1. Illustration of the developmental milestone for flexible PSCs from 2013 to 2018. This image gives the efficiency, configuration, interface and electrode for flexible perovskite devices. Copyright (2013, 2014, 2015, 2016, 2017) Royal Society of Chemistry; (2016, 2017, 2018) Wiley-VCH Verlag GmbH & Co. KGaA, Weinheim; (2015, 2016, 2017, 2018) American Chemical Society; (2014, 2015) Nature Publishing Group.

group mixed PbCl_2 and $\text{CH}_3\text{NH}_3\text{I}$ with a molar ratio of 1:3 and fabricated the perovskite layer via the one-step spin-coating method at room temperature.^[53] All of the spin-coating parameters, such as the speed, time, annealing temperature, and solvents used to dissolve the precursor, impact the perovskite film morphology.^[54] Grätzel and his co-workers investigated the influence of the annealing temperature on the formation of $\text{CH}_3\text{NH}_3\text{PbI}_3$ perovskite films by the one-step spin-coating method,^[55] and they found that the coverage of the film increased with the annealing temperature from 60 to 100 °C, but heterogeneous islands with big gaps in between were observed after further increasing the annealing temperature owing to the rapid formation of large sheets from various nucleation sites. Accordingly, the PSCs based on the absorber layer annealed at 100 °C yielded the highest PCE. The optimized low annealing temperature enabled the high-quality uniform perovskite films to be fabricated on flexible plastic substrates. The spin-coating speed and time directly determine the thickness of the absorber layer, and the thickness of the perovskite film needs to be about 300 nm for adequate light absorption in a good device.^[56–58] Considering the variation of the instrument parameters between different labs, the optimizations of the spin-coating conditions were performed individually.^[59–61] In the solution-processed methods, the solvents used to dissolve the precursor materials affect the morphology and crystalline properties during the formation of perovskites.^[62–65] The most commonly used solvents are *N,N*-dimethylformamide (DMF), dimethyl sulfoxide (DMSO), methyl-2-pyrrolidinone (NMP), *r*-butyrolactone (GBL), toluene, or a mixture of them.^[66–69] Seok and co-workers added toluene into a GBL/DMSO mixed solution and successfully fabricated extremely uniform and dense perovskite thin films via a MAI- PbI_2 -DMSO intermediate

phase, and a certified PCE of 16.2% without hysteresis was achieved for the devices based on the obtained perovskite films.^[70]

2.2. Two-Step Sequential Deposition

The one-step deposition technology using a mixture of PbX_2 and MAX in a common solvent leads to the uncontrolled precipitation of the perovskite, thus causing large morphological variations and resulting in a wide spread of photovoltaic performance in the resulting devices, which hampers the prospects for practical applications.^[71] Consequently, a low-temperature two-step deposition method was developed^[72] wherein the lead precursor is first coated onto the substrates, then MAI is introduced onto the surface of the obtained sample, usually by exposing it to the MAI solution.^[71] Through this method, the precursor materials can be converted into perovskite in a short time even at room temperature. Compared with that of their counterparts fabricated by one-step spin-coating methods, the morphology of the perovskite thin films used this two-step sequential deposition method is significantly improved, as shown in Figure 2, and the reproducibility of the performance of the corresponding PSCs is greatly increased.^[71] Huang et al. reported a different two-step deposition method to fabricate methylammonium lead triiodide (MAPbI_3) perovskite films by interdiffusion of spin-coated stacked layers of PbI_2 and MAI.^[73] They dissolved PbI_2 and MAI in DMF and 2-propanol, respectively, and then the layers were successively spin-coated onto the substrates to form the bilayer. The low temperature used is compatible with plastic flexible substrates. Although the two-step sequential solution-processed

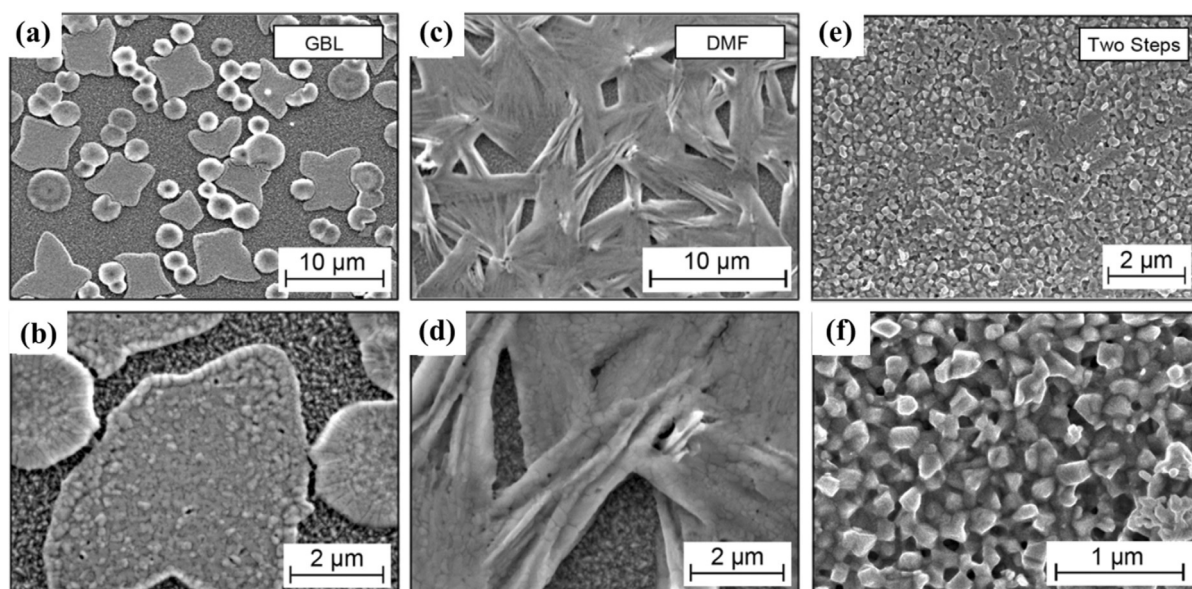


Figure 2. Comparison of perovskite thin films fabricated by one-step and two-step sequential deposition methods. a)–d) MAPbI_3 deposited by one-step spin-coating on a fluorine-doped tin oxide glass (FTO) substrate using a mixed solution of PbI_2 and MAI with molar ratio of 1:1 in (a,b) GBL or (c,d) DMF solvent. In both cases, the surface coverage is low, and bare FTO is exposed. e),f) MAPbI_3 obtained using the sequential deposition method. The dipping time of the PbI_2 film in the MAI 2-propanol solution was 30 s. Compared with the single-step method, the two-step sequential deposition yields much smaller MAPbI_3 crystallites and full coverage of the FTO surface.^[71] Copyright (2013) Science/AAAS.

deposition method provides an efficient low-cost route to high-performance PSCs, it still has some drawbacks: PbI_2 using this method cannot usually be converted completely, and the formation of the perovskite crystals cannot be controlled.^[74] Therefore, other modified deposition methods were developed to improve the PbI_2 conversion and morphology of the perovskite films.

For the solution-processed methods, additives offer an efficient way to improve the quality of the perovskite films.^[75] Researchers have developed and used many different additives in the precursor solution for the low-temperature perovskite fabrication procedure, such as polymers,^[76] full-erene,^[77] inorganic acid,^[78] solvents,^[51,79–81] and so on.^[82–84] To resolve the issue of poor coverage caused by the pristine $\text{MAPbI}_{3-x}\text{Cl}_x$, Su's group first added poly(ethylene glycol) (PEG) to the perovskite precursor solution to fabricate high-performance PSCs via a low-temperature process, and they found that the use of 1 wt % of PEG can cause a 25 % increase in the PCE.^[77] Subsequently, Zhao's group also used PEG as an additive in the precursor DMF solution and fabricated perovskite films via one-step solution-processed technologies under the mild temperature of 105 °C. The polymer-scaffold perovskite layer reinforces the architecture and improves strain tolerance, promising application in flexible devices. The efficiency of the novel PSC architecture based on an insulating polymer scaffold structure reached up to 16 %.^[78] Furthermore, the strong interaction between the PEG and perovskite molecule leads to resistance to humidity, thus enhancing the stability of the devices. Later, other polymer additives were developed to control the morphology and crystallinity of the perovskite films through the interaction between the long chains in the polymer networks and the perovskite molecules.^[75] Inorganic acid additives, such as hydriodic acid (HI), hydrobromic acid (HBr), and hydrochloric acid (HCl), have been developed to improve the performance of PSCs for their following advantages. First, they help increase the solubility of the perovskite precursor materials in the solvents. Second, they prevent perovskite decomposition by reducing I_2 formed into I^- ions.^[75] More importantly, the inorganic acid additives combine with PbI_2 to form a pre-crystallized intermediate complex, which then help to improve the perovskite crystal growth. It is found that the intermediate complex based on the inorganic acid significantly slows down the perovskite crystallization process, leading to improved crystalline quality because of inorganic acid difficult dissociation from PbI_2 . Therefore, inorganic acid additive is more effective in enhancing the perovskite grain size and crystalline structure, yielding high-quality perovskite film for higher solar cell performance. HI was first used as an additive in the perovskite precursor to increase the solubility of MAPbI_3 perovskite in DMF solvent. The addition of HI enabled the complete conversion of the PbI_2 into perovskite, therefore generating high-quality perovskite with pinhole-free and large crystal grains. The PSCs based on the as-prepared perovskite film show an average efficiency up to 17.2 % because of the improved charge-injection/separation efficiency, charge collection efficiency, diffusion coefficient, carrier lifetime, and reduced trap density.^[85] Surprisingly, water was used as an additive in the perovskite precursor

solution, although it has a low boiling point and high vapor pressure compared with other solvent additives such as 1,8-diodooctane (DIO)^[86,87] and 1-chloronaphthalene (CN).^[88] Grätzel et al. investigated how the water additive in the PbI_2 /DMF solution influences the properties of PbI_2 for perovskite films prepared using the two-step method. They found that the introduction of the water facilitates the formation of pinhole-free perovskite film with increased grain size and decreased defects, therefore enhancing the overall photovoltaic performance of the corresponding inverted solar cells.^[89] When water additive was introduced into the precursor solution during crystal perovskite growth, good crystallization and stability were also demonstrated. They concluded that $\text{MAPbI}_{3-x}\text{Cl}_x \cdot n\text{H}_2\text{O}$ hydrated perovskites were generated that enhanced the resistance to corrosion by water molecules to some extent. Accordingly, water-additive-based PSCs present a high PCE of 16.06 % and improved device stability under ambient conditions.^[90] Very recently, Yang et al. used dimethyl sulfide as an additive to slow down the perovskite crystal process, and achieved high quality perovskite films with larger crystal grains, lower trap density, and good environmental stability, leading to 19.61 % efficiency for rigid PSCs and 18.40 % record efficiency for flexible PSCs.^[51]

2.3. Other Low-Temperature Methods

Other efficient modified deposition methods were developed to improve the PbI_2 conversion and morphology of the perovskite films. Kelly et al. reported a modified two-step deposition technique with thermal evaporation used to prepare the PbI_2 precursor films, thus avoiding the problems caused by the solubility or viscosity of the PbI_2 precursor solution.^[91] They demonstrated that the thickness of the PbI_2 films can be precisely controlled and systematically varied by thermal evaporation, without any complications that accompany the spin-coating procedure.^[92] Afterwards, Yang's group developed a vapor-assisted solution-processed method to construct polycrystalline perovskite thin films with high quality. After the PbI_2 layer was spin-coated on the substrates from DMF solution, MAI powder was spread out around the PbI_2 coated substrates, which were then covered by a petri dish. After annealing at 150 °C, perovskite films with full surface coverage, small surface roughness, and grain size up to microscale were obtained.^[93] To solve the problems of incomplete conversion and limited solubility of the PbI_2 in the solution spin-coating methods, our group reported a different modified vapor-assisted technique. The PbI_2 was deposited on the substrates by vacuum evaporation, and a layer of MAI powder was placed on an aluminum plate. Then the PbCl_2 -coated samples were placed onto the MAI layer and heated to 150 °C to ensure the complete conversion of PbCl_2 , yielding perovskite films with full coverage.^[94]

3. Low-Temperature Interface Layers

The interface layers, including the electron transport layers (ETLs) and hole transport layers (HTLs), play key roles in high-efficiency PSCs. As interface layer materials requiring good properties, such as high transparency across the solar spectrum, high carrier mobility, and suitable energy level matching with the absorber layers, a crucial factor is that they can be fabricated by low-temperature technologies for flexible PSCs. In this section, we will separately review the ETLs and HTLs developed for flexible PSCs in the recent years.

3.1. Low-Temperature Electron Transport Layers

TiO₂ is the most popular electronic transport material used in PSCs because of its ideal Fermi level and large band gap.^[95,96] However, a fatal disadvantage of TiO₂ limits its application in flexible PSCs: TiO₂ films are usually deposited using spray pyrolysis or spin-coating techniques that require high-temperature (> 450 °C) sintering to achieve a relatively dense structure with good crystalline quality.^[97–101] Obviously, the high-temperature process not only complicates the fabrication procedures but is also incompatible with the polymeric substrates commonly used for flexible solar cells. To solve this problem, many low-temperature methods were developed to fabricate TiO₂.^[102–106] Nelles et al. reported a lift-off technique to transfer the pre-sintered TiO₂ layer to the desired substrates, thus avoiding the high-temperature process. Although the original electrical properties of the transferred porous layers are maintained, the fabrication procedure is too complicated to be widely used.^[107] Minor et al. used hydrothermal treatment of an aqueous mixed paste containing nanocrystalline TiO₂ powder and titanium salts to fabricate mesoporous nanocrystalline TiO₂ films at low-temperature (100 °C), but a PCE of only 2.3% was achieved for the flexible dye-sensitized solar cells, which is much lower than that using traditional high-temperature TiO₂.^[108] Jung et al. used the plasma-enhanced atomic layer deposition (PEALD) method to fabricate an approximately 20 nm-thick TiO_x compact layer at 80 °C. The efficiency of the flexible PSCs based on this low-temperature technology is up to 12.2%.^[109]

In 2015, our group demonstrated low-temperature TiO₂ films fabricated by magnetron sputtering at room temperature. The obtained dense amorphous TiO₂ film (named “am-TiO₂”) has a deeper Fermi level (−4.15 eV), enabling the electrons to be more easily injected into the TiO₂ film from the absorber layer, as shown in Figure 3 a–c. Owing to the advantages of am-TiO₂, including superior morphology, faster electron transport, and reduced transfer resistance, flexible PSCs using am-TiO₂ as ETLs on flexible poly(ethylene terephthalate) (PET)/ITO substrates were fabricated, and a PCE of 15.07% was achieved on a device with a respectably large area > 10 mm².^[94] Considering the complex synthesis conditions and sophisticated equipment needed, we subsequently developed a low-cost strategy for manufacturing an ETL. A solid-state ionic liquid (ss-IL) of 1-benzyl-3-methyl-

imidazolium chloride was introduced as an effective ETL by a solution-processed method at room temperature, as shown in Figure 3 d,e. We found that the ss-IL facilitates the reduction of the electron trap-state density at the perovskite absorber surface, therefore significantly eliminating the notorious hysteresis in the current-density voltage (*J*–*V*) curves. Also, because of the unique photoelectric properties of the ss-IL ETL, including its wide band gap, anti-reflection property, high electron mobility, and suitable work function (WF), the efficiency of the flexible PSCs based on the ss-IL ETL was further increased to as high as 16.09%.^[110] These works represent significant breakthroughs in the development of flexible PSCs.

To avoid the high-temperature problems, researchers developed other kinds of metal oxides at low temperatures to replace TiO₂, such as ZnO,^[111] SnO₂,^[50] ZnSnO₄,^[112] and W(Nb)O_x.^[113] It is known that one of the negative characteristics of PSCs is the low electron mobility of the conventional metal oxide ETL (10^{−4}–10^{−5} cm² V^{−1} s^{−1}) compared to the hole mobility of the frequently used HTLs.^[110,114] Because ZnO has an electron mobility substantially higher than that of TiO₂, and the ZnO nanoparticle layer can be deposited easily by spin-coating without a high-temperature heating or sintering step, it has become an ideal candidate for the ETL in flexible PSCs.^[115] In the initial report of flexible PSCs, Mathews et al. used ZnO as the ETL, which was fabricated by a chemical bath deposition (CBD) technique at 90 °C. Although the efficiency obtained was only 2.62%, the work provides a new perspective in the development of low-temperature interface layer materials.^[49] Subsequently, Liu and Kelly obtained a ZnO layer by spin-coating a butanol/chloroform mixture solution with a dispersion of ZnO nanoparticles onto the ITO substrate. The technique needs no calcination or sintering step. The efficiency of the flexible solar cells based on the relatively compact ZnO layer exceeded 10%.^[115] Later, Heo et al. used spin-coating and subsequent heat treatment at 150 °C to prepare ZnO layers for flexible PSCs and further enhanced the efficiency to 15.5%.^[116] Furthermore, e-beam-evaporated Nb₂O₅ is directly used by our group as an effective ETL without any post-treatment for PSCs. We found that Nb₂O₅ can serve as an effective carrier extraction layer and reduce the carrier recombination between the electrode and perovskite layer, and an efficiency of 15.56% was obtained for the flexible PSCs.^[117]

Recently, Yan et al. used PEALD technology to fabricate a SnO₂ thin film layer, and they found the charge transport of the SnO₂ layer can be efficiently improved after post-annealing in the presence of water vapor. They concluded that the water vapor can facilitate the complete reaction of organic materials upon the annealing process, leading to the formation of purer SnO₂. The efficiency based on the obtained SnO₂ layer reached 18.36% for the champion devices, which is among the highest values for flexible PSCs.^[50]

Apart from the metal oxides, some organic materials are used as the ETL because they can be fabricated by low-temperature methods, usually by spin-coating, making them easily compatible with the flexible substrates; such materials include 6,6-phenyl-C61-butyric acid methyl ester (PCBM),^[118]

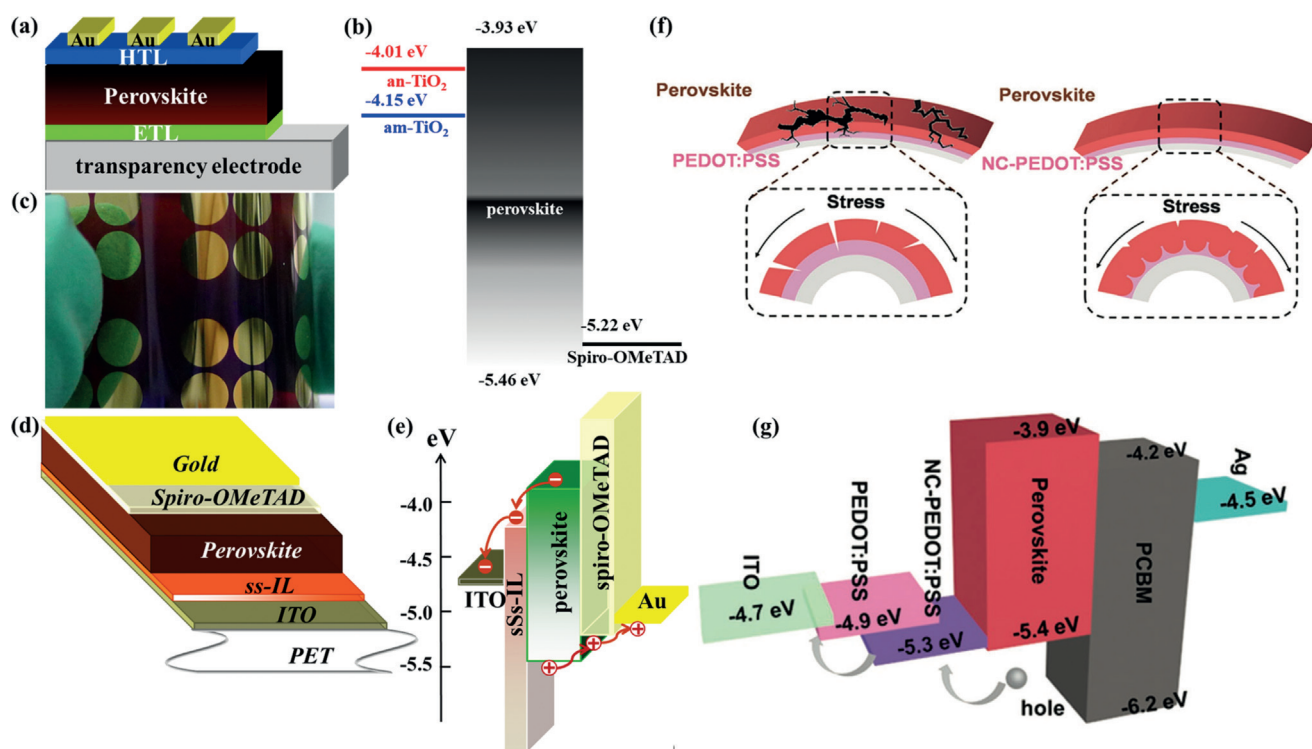


Figure 3. Low-temperature interface materials in flexible PSCs. a) The device structure of the planar PSC based on low-temperature TiO_2 (am- TiO_2). b) Energy-level diagram of the components of the PSC with anatase- TiO_2 (an- TiO_2) or am- TiO_2 as the ETL. The Fermi level of the am- TiO_2 decreased to -4.15 eV, facilitating electron injection into the am- TiO_2 from the perovskite absorber layer.^[94] c) A photograph of a flexible PSC using am- TiO_2 as the ETL. Copyright (2015) Royal Society of Chemistry. d) The structure of the flexible PSCs with ss-IL as the ETL. e) Energy-level diagram of the flexible PSCs, exhibiting the collection process of photo-generated charge carriers.^[110] Copyright (2017) Wiley-VCH Verlag GmbH & Co. KGaA, Weinheim. f) Stresses released by the NC-PEDOT:PSS HTL. The nanocellular scaffold can help release the mechanical stresses during flexural events, enhancing the repeatability and stability, with excellent flexural endurance for the flexible PSCs. g) Energy-level diagram of the PSC using NC-PEDOT:PSS as the HTL. The matched energy levels facilitate hole extraction from the perovskite layer and transfer to the anode.^[133] Copyright (2017) Wiley-VCH Verlag GmbH & Co. KGaA, Weinheim.

C_{60} ,^[119] *N,N*-bis(3-(dimethylamino)propyl)-*N,N'*-dimethylpropane-1,3-diamine (CDIN),^[120] and 1-benzyl-3-methylimidazolium chloride mentioned above,^[110] and so on.

3.2. Low-Temperature Hole Transport Layers

In flexible PSCs, one of the most commonly-used materials for HTLs is 2,2',7,7'-Tetrakis(*N,N*-di-4-methoxyphenylamino)-9,9'-spirobifluorene (spiro-OMeTAD) because its energy level is well-matched with those of perovskites, and the films can be easily fabricated via low-temperature methods.^[48,109,110] Although high efficiency has been achieved for flexible PSCs using spiro-OMeTAD as HTLs, there are still two unfavorable drawbacks: high cost and modest hole-mobility/conductivity.^[121–123] Therefore, other HTL materials have been developed to replace spiro-OMeTAD to improve the device performance. Poly(3,4-ethylenedioxythiophene)-poly(styrenesulfonate) (PEDOT:PSS), which is known to have a high WF and a positive influence on the built-in potential,^[124] usually with PCBM as the ETL, is especially used in inverted PSCs.^[125–128] A PCE of 9.2% has been obtained for the flexible PSCs with this very simple PET/ITO/PEDOT:PSS/perovskite/PCBM/Al structure.^[129] However,

the high acidity of PEDOT:PSS threatens to corrode the ITO electrode, leading to poor long-term device performance and stability when improperly encapsulated.^[130,131] To solve these problems, doped-PEDOT:PSS HTLs are being developed.^[132] For example, a polystyrene-doped nanocellular PEDOT:PSS (NC-PEDOT:PSS) HTL was fabricated via a low-temperature process. The novel nanocellular construction facilitates the release of the mechanical stresses during flexural events and shows significant feasibility for large-scale flexible PSCs, as shown in Figure 3 f,g. Owing to improved light harvesting, crystalline quality, and charge transport, a high efficiency of 12.32% for the MAPbI_3 -based flexible solar cells was achieved on a 1.01 cm^2 large area.^[133] Furthermore, the WF of PEDOT:PSS (4.9–5.2 eV) is very different from the valence band maximum energy of the perovskite (about 5.4 eV), leading to severe potential energy loss at the PEDOT:PSS/perovskite interface and reduced the built-in potential in PSCs, resulting in lower open-circuit voltage (V_{oc}).^[134,135] In fact, Lee et al. exploited self-organized polymer hole extraction layers to increase the built-in potential and thereby V_{oc} of the flexible PSCs.^[136]

Another method is to substitute other HTL materials for PEDOT:PSS in inverted PSCs, including small-molecule hole-transport materials (HTMs), organic polymer HTMs,

and inorganic HTMs.^[137–139] Owing to their defined molecular structures, tunable photophysical properties, and ability to be fabricated at low temperature for flexible solar cells, organic small-molecule HTMs have attracted enormous attention.^[139] Jin et al. designed and synthesized an organic small molecule, *N*-(4-(9*H*-carbazol-9-yl)phenyl)-7-(4-(bis(4-methoxyphenyl)amino)phenyl)-*N*-(7-(4-(bis(4-methoxyphenyl)amino)phenyl)-9,9-dioctyl-9*H*-fluoren-2-yl)-9,9-dioctyl-9*H*-fluoren-2-amine (CzPAF-TPA), as an HTL. The HTL showed an appropriate highest occupied molecular orbital (HOMO) energy level and high hole mobility. More importantly, the HTL can be fabricated by the solution-processed method and used in flexible PSCs, yielding an efficiency of 12.46%.^[139] Poly(triaryl amine) (PTAA) is known to be highly capable of increasing the device V_{oc} .^[140] Using PTAA as the HTL and low-temperature solution-processed ZnO as the ETL, flexible devices with a structure of poly-ethylenenaphthalate (PEN)/ITO/ZnO/MAPbI₃ perovskite/PTAA/Au were fabricated, yielding a PCE of 15.6%, with almost no hysteresis because of the good balance between the electron and hole conductivities in the ZnO ETL and PTAA HTL.^[138] Inorganic hole-transport materials, owing to their high mobility, low fabrication costs, and good chemical stability, have been employed to replace PEDOT:PSS layers in inverted perovskite devices.^[141] A solution-derived NiO_x film was employed as the HTL of a flexible PSC. The NiO_x film, which was spin-coated from a pre-synthesized NiO_x nanoparticles solution, can extract holes and block electrons efficiently without any other post-treatments. The low-temperature deposition process makes the NiO_x films suitable for flexible devices. NiO_x-based flexible PSCs were fabricated on ITO/PEN substrates, and a preliminary PCE of 13.43% was achieved.^[141] After a bis-C₆₀ surfactant was employed as an efficient ETL that aligns the energy levels at the organic/cathode interface, the efficiency for the NiO_x-based flexible solar cells reached 14.53%.^[142]

4. Flexible Electrodes

The electrodes used in flexible solar cells should possess several major strengths: high mechanical flexibility, good endurance, high conductivity and transparency, together with low sheet resistance. Until now, silver nanowires (Ag-NWs), Al-doped ZnO (AZO), ITO, carbon nanotubes, graphene, and organic materials have been used as the electrodes in flexible PSCs. Among the electrode materials that have been developed since the first report of flexible PSCs, ITO still maintains its predominance as a representation of conventional electrodes. To date, although the highest efficiencies are obtained from flexible PSCs based on ITO/PET substrates,^[50,94,110,143] it is apparent that the intrinsic brittleness of ITO causes a cracking problem that negatively influences the mechanical stability of the flexible devices,^[144] and the complicated fabrication process limits its application for commercialization.^[145]

To avoid these shortcomings, Ag-NWs have been demonstrated in flexible solar cells because of their outstanding optical and electrical properties, as well as their low-cost

solution-processed fabrication procedure.^[146] Jun et al. reported solution-processed Ag-NWs as a top electrode for flexible PSCs on titanium metal substrates. The flexible PSCs with the transparent and conductive Ag-NWs electrodes exhibited efficiency of up to 7.58%.^[147] The low efficiency is ascribed to the lower conductivity compared to that of ITO. Although other metal oxides^[148] and foils^[149] have been used, the flexible devices showed unsatisfactory performance. Bolink's group used AZO/Ag/AZO coated PET substrates in flexible PSCs and reported an efficiency of 7%,^[148] which is much poorer than that of ITO-based devices. Furthermore, other electrode materials have been developed, such as PEDOT,^[150] graphene, CNTs, and so on. PEDOT:PSS is known for high conductivity, transmittance and coverage, low sheet resistance, and easy fabrication by solution-processed methods. It has been reported that flexible PSCs incorporating PEDOT:PSS show good mechanical stability.^[151] Kelly and co-workers found that the device deterioration after repeated bending results mainly from cracks appearing in the metal oxide electrodes. To clarify this point, they fabricated flexible PSCs on PET substrates using transparent PEDOT:PSS and others using metal oxide (In₂O₃) electrodes. The fatigue measurements showed that after bending the devices over a cylinder with a 4 mm radius for up to 2000 cycles, the PEDOT:PSS electrodes showed negligible change in their sheet resistance, and therefore maintained better device performance, while the metal oxide electrodes appeared to have obvious cracks, leading to an extremely high sheet resistance and device failure, as shown in Figure 4a–d.^[151] However, as mentioned previously, PEDOT:PSS easily suffers from water erosion, which is a dangerous threat to device stability.^[150] Owing to its high optical transmittance, high charge mobility, and electronic conductivity, as well as excellent chemical stability, graphene is considered one of the most appealing candidates for photovoltaic devices.^[152] In 2016, Yan's group first used graphene transparent electrodes in flexible PSCs. An efficiency of 11.5% was obtained for the flexible devices with the configuration of polyethylene terephthalate/graphene/poly(3-hexylthiophene)/MAPbI₃/PC₇₁BM/Ag, wherein poly(3-hexylthiophene) (P3HT) was used as the HTL to improve the stability.^[153] To further lower the sheet resistance and introduce chemical bonding between the graphene layer and PET substrate, chemical doping methods were used. Choi et al. improved the efficiency to 16.8% by using a MoO₃-modified graphene layer in flexible PSCs.^[154] As shown in the Figure 4e–g, the sheet resistance of the PEN/ITO film increased by nearly five times the initial value after 1000 bending cycles. When the metal thin films were formed on the graphene as contact pads for wire-bonding, linear cracks would generate on the metal electrodes due to weak adhesion between the graphene and the metal surfaces. Im et al. found AuCl₃-doping efficiently reduced the sheet resistance of the graphene single layer on the PET substrate and improved the efficiency to 17.9%.^[155]

As another ideal alternative electrode material for flexible photovoltaics, carbon nanotubes (CNTs) have been investigated because of their high electrical conductivity and optical transparency, which result from their network of

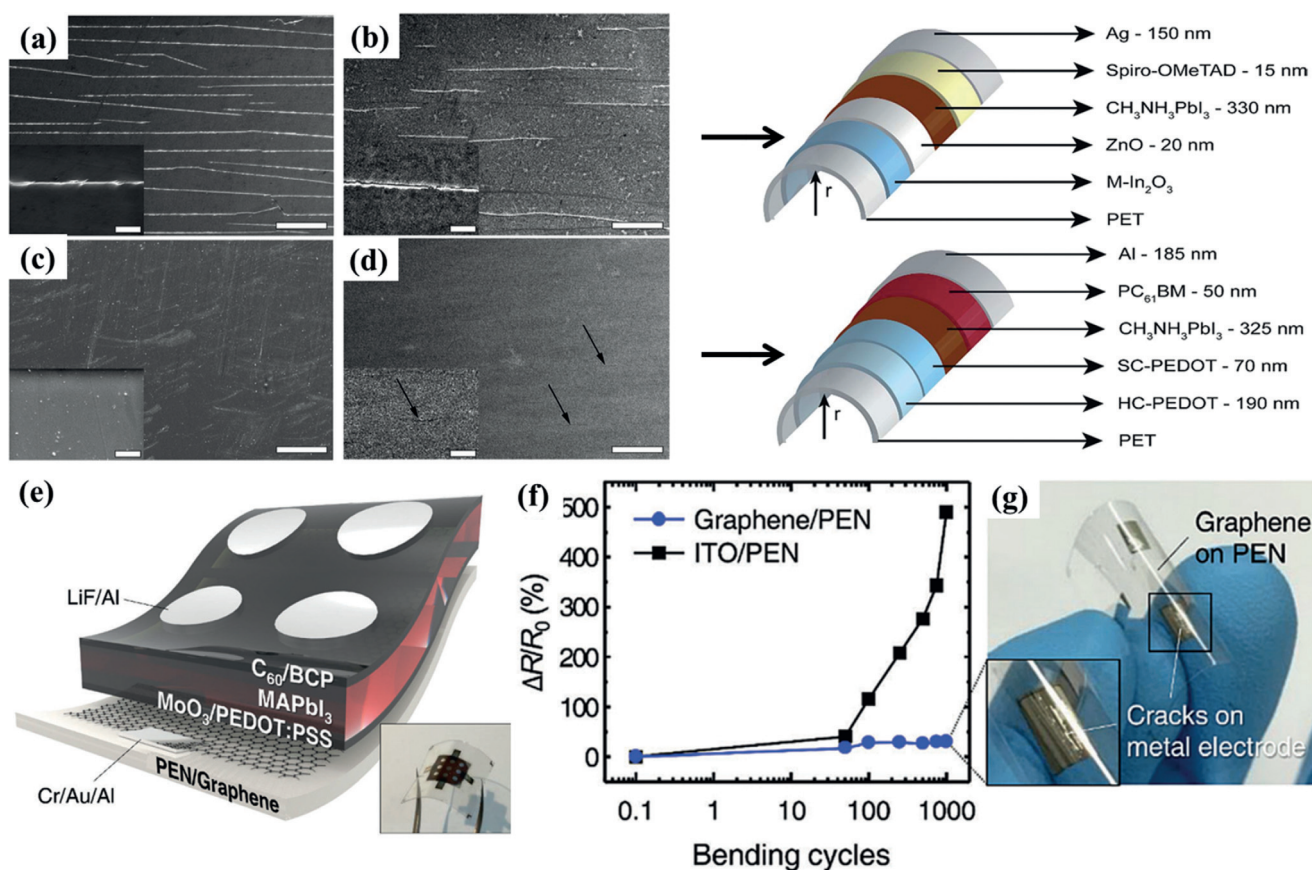


Figure 4. Flexible solar cells using different electrode materials. SEM images of a) PET/M-In₂O₃, b) PET/M-In₂O₃/ZnO/MAPbI₃, c) PET/HC-PEDOT, and d) PET/HC-PEDOT/SC-PEDOT/MAPbI₃ films after 2000 bending cycles. On the right are schematics of the corresponding device architectures for M-In₂O₃/ZnO/MAPbI₃ and HC-PEDOT/SC-PEDOT/MAPbI₃ cells. The insets are magnified images. The scale bars in the main and inset images are 50 mm and 5 mm, respectively. The locations of the small cracks in the perovskite layer are marked by arrows in (d).^[151] Copyright (2015) Royal Society of Chemistry. e) Device structure of graphene-based flexible PSCs (inset image: Photograph of a complete device). f) Relative resistance change ($\Delta R/R_0$) of the Gr-Mo/PEN and ITO/PEN films as a function of bending cycles at $R=4$ mm. g) Photograph of a Gr-Mo/PEN substrate on which rectangular Al/Au/Cr electrodes were formed. When the substrate was bent twice at $R=4$ mm, linear cracks were generated on the metal electrodes due to weak adhesion between the graphene and the metal surfaces.^[154] Copyright (2017) Royal Society of Chemistry.

essentially infinitely conjugated double bonds.^[156] In 2015, a transparent CNTs electrode was used in flexible PSCs on titanium foil substrate.^[157] To make a comparison, Matsuo's group fabricated inverted flexible PSCs with CNT and others with graphene as electrodes. They found that both kinds of flexible PSCs showed high reproducibility with no hysteresis. However, the graphene-based flexible devices performed better because of their superior morphology and higher transparency.^[156] Furthermore, CNTs have been demonstrated as the cathode in fiber-shaped^[158] and inverted flexible PSCs.^[159]

From the above sections, it can be seen that PSCs are ideal for flexible solar cells, owing to the unique quality of perovskite materials, low-temperature film deposition techniques, including perovskite film, ETL, HTL, and flexible electrodes. Table 1 summarizes important developments of flexible PSCs, including device structures, solar cell types, key improvement, and photovoltaic parameters, including V_{oc} , J_{sc} , fill factor (FF), and PCE. It is apparent that the efficiency rapidly increased from 2.62% to 18.4% in just 5 years,

indicating that perovskites possess enormous potential in flexible photovoltaics.

5. Stability of Flexible Perovskite Photovoltaics

In flexible PSCs, there are two kinds of stabilities related to the flexible PSCs. One is mechanical stability, which is often limited by the mechanical robustness of electrodes. Another is long-term environmental stability, which is determined by perovskite absorbers and interfacial layers.

5.1. Mechanical Stability of Flexible PSCs

In general, ITO coated flexible polymer substrates, such as PET and PEN, are used as electrodes in high-efficiency flexible solar cells. Compared to the ITO coated rigid glass substrates, the main disadvantages of ITO on the flexible polymer substrates are originated from relatively low con-

Table 1: Summary of the key developments in the history of flexible PSCs.

Device structure	Type	Key improvement	V_{oc} [V]	J_{sc} [mAcm ⁻²]	FF [%]	PCE [%]	Ref.
ITO-free							
Ti/dimple c-TiO ₂ /mp-TiO ₂ /MAPbI ₃ /Spiro-OMeTAD/Ag NW	normal	Spray coated Ag NWs	0.73	12.0	44.0	3.85	[196]
PET/PEDOT:PSS/MAPbI ₃ /TiO ₂ /Al	inverted	Spray coated PEDOT:PSS	0.75	15.8	41.0	4.90	[197]
PET/SWCNT/MAPbI ₃ /PCBM/Al	inverted	HNO ₃ doped SWCNT	0.71	11.8	56.0	5.38	[198]
Ti/c-TiO ₂ /mp-TiO ₂ /MAPbI ₃ /Spiro-OMeTAD/ultra-thin Ag	normal	Semi-transparent	0.89	9.5	72.8	6.15	[199]
PET/AZO/Ag/AZO/PEDOT:PSS/Poly-TPD/MAPbI ₃ /PCBM/Au	inverted	AZO/Ag/AZO	1.04	14.3	47.0	7.00	[111]
PET/PEDOT:PSS/MAPbI ₃ /PCBM/Al	inverted	High conductivity PEDOT	0.80	15.0	60.0	7.60	[151]
PET/Ag nano-network/graphene oxide/PEDOT:PSS/MAPbI ₃ /PFN-P1/PCBM/Ag	inverted	PFN-P1 ETL	0.94	12.7	66.2	7.92	[200]
Ti/TiO ₂ nanotubes/MAPbI ₃ /Spiro-OMeTAD/CNT	normal	TiCl ₄ treated TiO ₂ nanotubes	0.99	14.4	68.0	8.31	[157]
PET/PEDOT:PSS/PEI/MAPbI ₃ /Spiro-OMeTAD/Au	normal	PEI-modified PEDOT:PSS	0.95	17.2	59.7	9.73	[201]
Ti-foil/c-TiO ₂ /mp-Al ₂ O ₃ /MAPbI _{3-x} Cl _x /Spiro-OMeTAD/PEDOT:PSS/PET with Ni mesh	normal	Transparent conductive and adhesive counter electrode	0.98	17.0	61.0	10.30	[149]
NOA63/PEDOT:PSS/MAPbI ₃ /PCBM/Eutectic Ga-In blend	inverted	Shape recoverable cell	0.92	16.6	70.5	10.75	[202]
PET/AZO/ZnO/C60/MAPbI ₃ /Spiro-OMeTAD/MoO ₃ /In ₂ O ₃ :H embedded with Ni/Al grid	normal	Thermally evaporated C60 and MoO ₃	1.08	16.1	68.6	12.20	[203]
Cu/CuI/MAPbI ₃ /ZnO/Ag nanowires	inverted	Spray coated Ag nanowires	0.96	22.5	59.2	12.80	[168]
Ti/TiO ₂ nanowire/MAPbI ₃ /PEDOT/PEN-ITO	normal	Spin-coated TiO ₂ nanowire	0.94	21.7	63.0	13.07	[204]
PET/IZO/TiO ₂ /MAPbI ₃ /Spiro-OMeTAD/Ag	normal	Spin-coated TiO ₂ nanoink	1.05	18.2	70.0	13.20	[176]
PET/Ag-mesh/PH1000/PEDOT:PSS/MAPbI ₃ /PCBM/Al	inverted	Ultralight (1.96 W/g)	0.91	19.5	80.0	14.00	[205]
PEN/Graphene-Mo/PEDOT:PSS/MAPbI ₃ /C60/BCP/LiF/Al	inverted	CVD deposited graphene	1.00	21.7	80.0	16.80	[154]
ITO Electrode							
PET/ITO/c-ZnO/ZnO nanorod/MAPbI ₃ /Spiro-OMeTAD/Au	normal	Electrodeposited ZnO	0.80	17.5	43.1	2.62	[49]
PEN/ITO/PEDOT:PSS/FASnI ₃ /C60/BCP/Ag	inverted	Pb-free	0.31	16.1	62.6	3.12	[206]
PET/ITO/ZnO/MAPbI ₃ /Carbon	normal	Blade coated carbon paste	0.76	13.4	42.0	4.29	[207]
PET/ITO/PEDOT:PSS/MAPbI _{3-x} Cl _x /PCBM/ZnO/Ag	inverted	Fully slot-die cell	0.90	10.9	50.0	4.90	[188]
PET/ITO/PEDOT:PSS/MAPbI ₃ /PCBM/Bis-C60/Ag	inverted	Blade coated all active layers	0.87	13.9	59.0	7.14	[208]
PET/ITO/TiO ₂ /MAPbI _{3-x} Cl _x /Spiro-OMeTAD/Ag	normal	Ultrasonic spray-coated perovskite	1.03	15.3	51.4	8.10	[170]
PET-ITO/Ti/MAPbI ₃ /Spiro-OMeTAD/Ag	normal	RF sputtered metallic Ti ETL	0.83	15.2	66.0	8.39	[162]
PET/ITO/c-TiO ₂ /mp-TiO ₂ /MAPbI ₃ /Spiro-OMeTAD/Au	normal	Plasma ALD deposited TiO ₂	0.88	14.9	70.0	9.20	[209]
PEN/ITO/TiO ₂ /MAPbI ₃ /CNT	normal	Chemical vapor deposited CNTs	0.91	15.9	65.6	9.49	[210]
ITO/MAPbI ₃ /PCBM/Al	inverted	ETL free	0.96	14.8	68.1	9.70	[211]
PET/ITO/ZnO/MAPbI ₃ /Spiro-OMeTAD/Ag	normal	Spin-coated ZnO nanoparticles	1.03	13.4	73.9	10.20	[115]
PET/ITO/ZnO/MAPbI ₃ /Spiro-OMeTAD/Au	normal	Sputtered ZnO	0.87	19.2	67.6	11.29	[212]
PEN/ITO/MAPbI ₃ /Spiro-OMeTAD/MoO ₃ /Ag	normal	Gas pump drying	0.96	17.4	56.0	11.34	[213]
PET/ITO/Zn ₂ SnO ₄ /PCBM/MAPbI ₃ /Spiro-OMeTAD/Ag	normal	Spin-coated Zn ₂ SnO ₄ ETL	1.05	17.4	63.8	11.61	[214]
PEN/ITO/NiO _x /MAPbI _{3-x} Cl _x /PCBM/BCP/Ag	inverted	Spin-coated NiO _x nanoparticle	1.04	17.7	64.2	11.84	[169]
PEN/ITO/TiO _x /MAPbI _{3-x} Cl _x /Spiro-OMeTAD/Ag	normal	ALD deposited TiO ₂	0.95	21.4	60.0	12.20	[109]
Flexible glass/ITO/ZnO/MAPbI ₃ /Spiro-OMeTAD/Au	normal	PDMS anti-reflection layer	0.98	19.3	69.0	13.14	[26]
PEN/ITO/PEIE/C60/MAPbI ₃ /Spiro-OMeTAD/Ag	normal	Evaporated C60	1.02	17.9	73.0	13.30	[215]
PET/ITO/NiO _x /MAPbI ₃ /PCBM/Ag	inverted	Spin-coated NiO _x nanoparticle	1.04	18.7	68.9	13.43	[141]
PET/ITO/TiO ₂ /MAPbI _{3-x} Cl _x /PTAA/Au	normal	Electron beam evaporated TiO ₂	0.91	21.3	69.0	13.50	[216]
PEN/ITO/SnO ₂ /PCBM/MAPbI ₃ /Spiro-OMeTAD/Au	normal	PLD deposited SnO ₂	1.08	20.6	63.0	14.00	[217]
AgNW-GFRHybrimer/c-ITO/PEDOT:PSS/MAPbI ₃ /PCBM/BCP/Ag	inverted	Evaporated BCP	0.99	21.5	66.0	14.15	[218]
PET/ITO/NiO _x /MAPbI ₃ /C60/Bis-C60/Ag	inverted	Spin-coated NiO _x	1.00	20.9	69.6	14.19	[219]
PET/ITO/Al ₂ O ₃ /MAPbI ₃ /Spiro-OMeTAD/Au	normal	ALD deposited Al ₂ O ₃	1.00	22.8	67.0	14.60	[220]
PET/ITO/Li:SnO ₂ /MAPbI ₃ /Spiro-OMeTAD/Au	normal	Li doped SnO ₂	1.02	20.6	76.3	14.78	[221]
PET/ITO/TiO ₂ /MAPbI _{3-x} Cl _x /Spiro-OMeTAD/Au	normal	Sputtered TiO ₂	1.03	20.9	70.0	15.07	[94]
PET/ITO/Zn ₂ SnO ₄ /MAPbI ₃ /PTAA/Au	normal	Spin-coated Zn ₂ SnO ₄ nanoparticle	1.05	21.6	67.0	15.30	[112]
PI/ITO/ZnO/MAPbI ₃ /PTAA/Au	normal	Roll-to-roll sputtered ITO	1.10	17.6	79.4	15.40	[167]
PEN/ITO/ZnO/MAPbI ₃ /PTAA/Au	normal	Spin-coated ZnO nano-sol	1.10	18.7	76.0	15.50	[116]
PET/ITO/Nb ₂ O ₅ /(FAPbI ₃) _{0.85} (MAPbBr ₃) _{0.15} /Spiro-OMeTAD/Au	normal	E-beam evaporated Nb ₂ O ₅	1.12	23.5	63.1	15.56	[117]
PEN/ITO/W(Nb)O _x /MAPbI _{3-x} Cl _x /Spiro-OMeTAD/Ag	normal	W(Nb)O _x Modified by Nb ⁵⁺	0.98	21.4	75.0	15.65	[113]
PEN/ITO/c-TiO ₂ /BK-TiO ₂ /MAPbI ₃ /Spiro-OMeTAD/Au	normal	Electro-deposited TiO ₂	1.07	19.5	75.0	15.76	[119]
PET/ITO/TiO ₂ /MAPb(I _{1-x} Br _x) ₃ /PTAA/Au	normal	RF sputtered TiO ₂	1.11	20.8	69.0	15.88	[222]

Table 1: (Continued)

Device structure	Type	Key improvement	V_{oc} [V]	J_{sc} [mA cm ⁻²]	FF [%]	PCE [%]	Ref.
PET/ITO/ss-IL/(FAPbI ₃) _{0.85} (MAPbBr ₃) _{0.15} /Spiro-OMeTAD/Au	normal	Solid-state ionic liquid	1.07	22.7	66.2	16.09	[110]
PEN/ITO/ PEDOT:PSS/MAPbI ₃ /C60/BCP/LiF/Al	inverted	Vacuum thermal evaporated ETL	0.97	21.5	83.0	17.30	[154]
PET/ITO/SnO ₂ /C60-SAM/MA _{1-x} FA _x PbI ₃ /Spiro-OMeTAD/Au	normal	Pb(SCN) ₂ additive	1.08	22.2	75.1	17.96	[223]
PET/ITO/PTAA/FAPb _{1-x} Br _x /PCBM/C60/BCP/Cu	inverted	Cu electrode	1.06	22.8	74.6	18.10	[143]
PET/ITO/treated SnO ₂ /C60-SAM/MA _{1-x} FA _x PbI ₃ /Spiro-OMeTAD/Au	normal	Water treated SnO ₂	1.10	22.1	75.4	18.36	[50]
PET/ITO/Nb ₂ O ₅ /MAPbI ₃ /Spiro-OMeTAD/Au	normal	Dimethyl sulfide additive	1.10	22.5	74.2	18.40	[51]

ductivity, smaller transmittance and poorer mechanical robustness.^[160,161] It is well known that the commonly-used polymer substrates cannot survive high temperature processing beyond 250 °C. Therefore, all depositions and treatments have to be done at lower temperature, leading to inferior ITO resistivity (more than 20 Ω/sq).^[51] To compensate the low conductivity, thicker ITO coatings are used to improve the conductivity. In fact, the thickness of commercial ITO coating on PET is over 400 nm, while it is only 150 nm for the ITO coating on glass. The thicker ITO coating causes compromised transmittance, leading to lower short-circuit current density (J_{sc}) and PCE. The substrate flexing after device fabrication will normally lead to some performance loss as well. As a result, the efficiency of flexible PSCs is often lower than that of the rigid perovskite devices.

Meanwhile, the mechanical bending stability is an important indicator in flexible PSCs. Seok's group reported the efficiency of flexible PSCs based on PEN/ITO degraded by only 5% of its initial efficiency after 300 bending cycles.^[112] Jung et al. also reported a flexible perovskite device based on the same substrates with a PCE of 12.2%, but 50% loss of initial efficiency was observed after 1000 bending cycles under bending radius of 10 mm.^[109] Carlo et al. found that it is safe for ITO to be bended to a radius of 14 mm, and when the bending radius is smaller than 14 mm, the ITO coating starts to crack, leading to significant degradation in conductivity.^[162] To examine the intrinsic mechanical stability of the flexible PSCs, Liu et al. adopted different bending radius to test the flexible perovskite device based on the PET/ITO substrates.^[163] The efficiency of flexible device shown negligible degradation when flexed at bending radius of 14 mm for 500 cycles, however, the PCE displayed severe drop when bending radius was smaller than 14 mm, in good agreement with a previous report.^[163] Very recently, by using a thin silver layer sandwiched in between ITO coatings on PET substrates, Yang et al. managed to effectively reduce the ITO thickness while warranting high conductivity and mechanical bending robustness,^[51] achieving record efficiency 18.40%, and bending measurements revealed that the PCE remained 83% of its initial efficiency even bending radius was reduced to 4 mm.^[51] Furthermore, other flexible electrodes, such as Ag-NWs, carbon, graphene, conducting polymer, etc. are better ways to improve mechanical stability of flexible PSCs.

5.2. Environmental Stability and Encapsulation for Flexible PSCs

Long-term environmental stability is a critical standard to evaluate solar cells for practical applications. Unfortunately, it remains to be a challenge for the PSCs to date. Generally, the instability is derived from environmental sensitivity of HTLs and perovskite degradation. Until now, spiro-OMeTAD, PTAA and PEDOT:PSS are frequently used as HTLs in flexible PSCs due to the low temperature and easy fabrication. Some additive like bis(trifluoromethanesulfonyl) imide (TFSI) and tert-butylpyridine (*t*BP) are employed to enhance conductivity and improve performance.^[164] Nonetheless, perovskite would corrode by *t*BP, and degradation by moisture sensitive TFSI.^[165,166] Furthermore, the moisture-sensitive PEDOT:PSS would lead to poor stability of flexible PSCs.^[132] Some stable hole-transport materials fabricated at low temperature, such as NiO, CuI, poly(3-hexylthiophene) (P3HT), etc.,^[167-170] have been developed to replace the commonly used HTLs. The stability and performance of flexible PSCs have been improved using these HTLs.

Perovskite absorber is very sensitive to humidity, oxygen, and UV light, resulting in degradation and phase transition of perovskite in flexible devices. For example, MAPbI₃ degrades into PbI₂ and MAI when exposed in ambient air.^[171] While formamidinium-based lead triiodide (FAPbI₃) occur phase transition from black α -phase to yellow δ -phase once it is exposed to moisture.^[172] In view of the stability issue for industrialization, encapsulation technology becomes an imperative tool to isolate the sensitive cells from corrosive ambient. For flexible PSCs, the effective encapsulation is of a great challenge. The polymeric PEN and PET substrates not only exhibit high water vapor transmission rate (WVTR; about 18 gm⁻²day⁻¹ for PET at 37 °C and 90% relative humidity),^[164] but also display severe oxygen infiltration (0.462 cc(STP) cm m⁻² day⁻¹ for PET).^[173] As a result, encapsulation is required for both the front and back sides for flexible PSCs. For the front active area side, flexible sealing film with low WVTR and small oxygen infiltration can be employed to cover the surface. The back side also needs to be encapsulated by flexible materials with high transmittance, low WVTR, and small oxygen infiltration. Atomic layer deposition (ALD), physical vapor deposition (PVD), plasma enhanced chemical vapor deposition (PECVD) and other technique of metal oxides have been demonstrated as efficient methods to seal the back side.^[174,175] For example, Weerasinghe et al. systematically studied the encapsulation of

flexible PSCs exposed in humidity of 30–80% for 500 h. It was found that the flexible PSCs with complete encapsulation remained the initial efficiency after 500 h, and the devices with partial encapsulation were obviously decayed after 400 h, while the flexible devices without encapsulation shown severe degradation in just 100 h.^[176] These results demonstrate that the effective encapsulation is essential for flexible PSCs.

6. Flexible Perovskite Photovoltaics Applied in Portable Electronic Devices

Wearable devices have played an important role in the consumer electronic market, such as to monitor people's physical condition or to record people's sport information. However, the most important issue of wearable devices is the low energy source. The high efficiency of flexible PSCs potentially enable the wearable device to work continuously even if there are no batteries or only small capacity batteries are required as the backup power. Recently, it was also found that PSCs exhibit excellent dim-light performance, and the efficiency of rigid PSCs exceeds 27% indoor light, that means the flexible PSCs promising power source for wearable devices under indoor conditions.^[177,178] Typically, household lighting ranges from 100 to 1000 lux. These illuminances correspond to 31–310 μWcm^{-2} light intensity with a 6500 K fluorescent lamp spectrum. Assuming 20% efficiency could be achieved for a flexible cell, it means that 100 mW power output requires less than 1800 cm^2 , which is available in a bag or clothes. This energy is enough to power some wireless sensors, portable electronics and internet of things. Amazingly, it could be fabricated to some wearable flexible devices, such as hats, clothes or bags, thanks to the softness of perovskite materials.

Here we demonstrate some cases that flexible PSCs applied in portable electronic devices, as shown in Figure 5. A bag could be covered by flexible cells for both sides to enlarge illumination area and generate a higher power. As a result, it could be not only the power source for smart phones even under ambient light indoors, but also allow the portable devices to be powered outdoors.

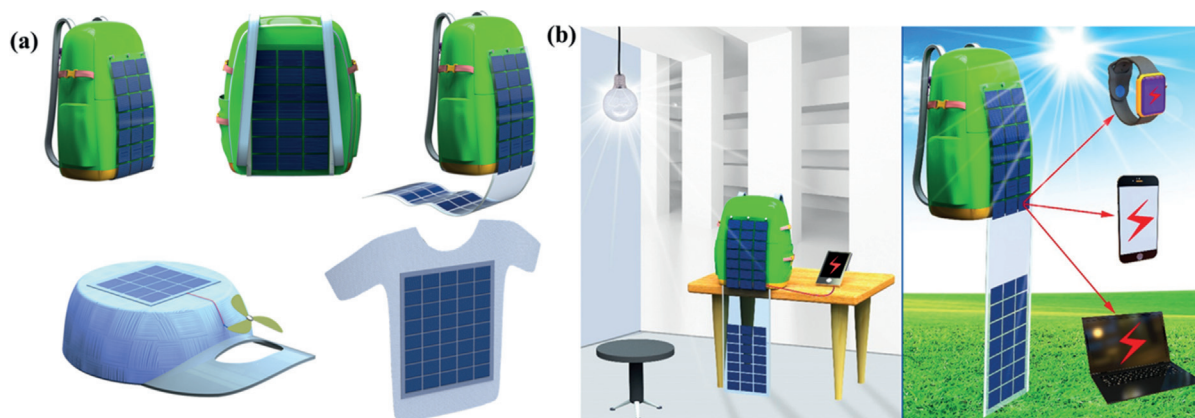


Figure 5. Illustration of flexible PSCs integrates with some wearable devices. a) Bag with both sides covered by flexible perovskite devices, and wearable devices for flexible PSCs provide the power in hat and clothes. b) Cases of indoor and outdoor situations for the perovskite-based flexible solar-cell-covered bag to charge smart phones, smart watches, and laptops.

7. Potential Commercialization

As a new burgeoning clean technology, the feasibility of commercialization of the PSCs is one of the most concerned topics since its appearance. We developed an alternating vacuum-deposition method to fabricate the high quality perovskite films, providing a qualified way to promote the industrial realization.^[40,179] Compared with the solution processing that easily generates incomplete surface coverage, especially for larger scale films, cause solvent inclusion and moisture penetration, the vacuum deposition method provides high quality perovskite films with full surface coverage, smaller roughness, and more uniform morphology, along with crystalline phases of higher purity. Because the vacuum deposition environment offers better moisture protection, the devices show excellent stability and high efficiency with minimum performance variation. Moreover, unlike the traditional vacuum deposition method that requires to monitor and control the deposition rates, the alternative layer deposition technology relaxes the complicated operations. For larger-scale perovskite device fabrication, the key point is to remain the quality of the perovskite film such as uniform and coverage. Hopefully, the combination of vacuum deposition methods and the low-temperature techniques offers a promising way to realize the mass production of the flexible PSCs.

Another cost-effective way to realize the mass production of flexible PSCs is continuous roll-to-roll technology, that feeds devices on a roll of flexible substrates.^[180] As is known for its focus on potential large-scale fabrication processes, roll-to-roll processing has been successfully implemented in solar cell fabrication, especially in the field of organic solar cells^[181] and dye sensitized solar cells.^[182] Compared to present solar cells, the perovskite photovoltaics are more convenient to develop large-scale flexible devices using roll-to-roll technology, because of excellent properties of perovskite materials, such as high absorption coefficient, good solubility in polar solvent, and super mechanical toughness.^[183–185] Furthermore, fabrication of flexible PSCs by roll-to-roll technology is expected to be successfully owing to the simple device structure and opportune manufacturing process.^[185] Usually, the flexible substrates used in this technique

to fabricate large scale PSCs is PET or PEN, because of the good transmission that promise the incident light transformed into the perovskite absorber layer. Considering the process temperature required for the fabrication of all the functional layers incorporated in the device configuration, printing or coating techniques could be mounted into a roll-to-roll system to produce the perovskite active and carriers transport layers.^[186] The back electrodes can be deposited through screen printing and roll-to-roll vacuum techniques. Thus far, a few achievement has been obtained on the fabrication of PSCs through the roll-to-roll processing.^[187–189] For example, Huang's group used roll-to-roll system with slot-die coating to fabricate fully-printable PSCs, yielding a PCE of 11.96% with an active area of 10 mm².^[187] Though the active area is far from enough to be considered into the real application, this work highly demonstrated the PSCs are compatible with roll-to-roll processing. Furthermore, more work is needed to be developed to optimize the continuous roll-to-roll fabrication process parameters to realize the commercialization of PSCs with high efficiency and stability PSC commercialization, such as the solvent selection, deposition speed and flow, substrate and annealing temperature, and film thickness.

In 2014, about 40 GW of photovoltaic modules have been installed globally, 92% of which were crystalline silicon solar cells.^[190] However, the cost of the electricity generated from these modules is still higher compared with that provided by the traditional fossil fuels.^[191] Because of the abundance of relatively cheap precursor materials and the potential ultra-low-cost production of PSCs, as well as the attractively high efficiency, researchers believed that the PSCs modules will be a leader in the future photovoltaic market. Han's group evaluated the manufacturing costs of the PSC modules based on two kinds of structures, with module A fabricated mainly by screen printing and module B by lasers and vacuum evaporation to achieve a high efficiency of 19%.^[190] To provide a comparison with other photovoltaic technologies, they made detailed calculation on the costs of capital amortization, materials and overhead cost. And they found that the manufacturing costs for the PSC models were one third of that based on bulk silicon PV technologies. More importantly, the leveled cost of the electricity produced from these modules could be competitive with that from the fossil fuels, as low as 6 UScents/KWh, proposed in the U.S. SunShot Initiative if the module efficiency and lifetime exceeded 12% and 15 years, respectively. Based on these results, we believe that the combination of developed alternated vacuum deposition technology with the roll-to-roll system can hopefully realize the ultra-low-cost of PSCs manufacture.

8. Conclusion and Outlook

Flexible PSCs have attracted significant attention because they are suitable for mass-production by roll-to-roll fabrication techniques, promising huge potential for practical applications in light, wearable, and portable electronic devices. Both the low cost and accessibility of the precursor materials for the perovskites and the easy formation of the

thin films by low-temperature methods give fundamental support for the use of perovskites in flexible solar cells. Undoubtedly, the high quality of the perovskite thin films, including uniform morphology, full coverage, highly oriented crystalline structure, and suitable band gap, are prerequisites for high efficiency flexible PSCs. As mentioned above, several different kinds of methods have been developed to optimize the properties of the perovskite thin films, such as by tuning the proportion of the components incorporated in the perovskite structure or by modifying the fabrication technologies. More recently, perovskite quantum dots have been developed as an effective absorber material owing to some special characteristics and a high specific surface area, which makes perovskite quantum dots promising candidates for photovoltaic and optoelectronic applications.^[192] Up to now, flexible light-emitting diodes,^[193] flexible nonvolatile memory^[192] based on perovskite quantum dots have been reported with promising performance. In particular, all inorganic cesium lead halide perovskite quantum dots have been successfully applied in rigid PSCs, with an efficiency of over 13%.^[194,195] Even though there has been no report on quantum-dot-based flexible perovskite solar cells, its low-temperature processing makes it a possible alternative for flexible PSCs.

Apart from the absorber materials, the flexible interface layer and the electrodes also play indispensable roles in improving the performance of the devices. Researchers have made great efforts to develop ETLs, HTLs and electrode materials, and significant achievements have been made, with the efficiency increased to over 18% in just a few years. However, three issues still challenge the further development of flexible PSCs for practical application: limited flexibility, unfavorable bending stability, and reduced efficiency on a large scale.

Conventional high-efficiency flexible perovskite devices are fabricated on ITO/PET or PEN substrates. However, the rigid characteristic of ITO causes cracks in the thin film, which is the main reason for device failure after repeated bending, and most bending tests are carried out with a bending radius of more than 1 mm or for limited bending cycles, neither of which is sufficient for claiming good bending tolerance. The same problems are seen in the flexible PSCs based on other metal oxides or metal foil substrates. Therefore, carbon materials such as graphene and CNTs, and organic materials such as PEDOT:PSS, were used to avoid these cracking problems. Although the efficiency is much poorer than that of devices using ITO (because of the high sheet resistance and lack of bonding between the electrode layer and plastic substrates), they provide a promising means to improve the bending stability, which is a vital parameter for flexible PSCs in practical applications.

To date, almost all reported flexible PSCs have small areas. It is well known that the PCE is reduced when the area of the devices is increased to large scale, owing to the inevitable loss of homogeneity in the films. As a result, the deposition process for the thin films at large scale directly determines the performance of the large-area flexible PSCs. Therefore, large-area techniques need to be developed for the fabrication of all the layers in flexible solar cells. Therefore,

the alternated vacuum deposition technology should be introduced into the roll-to-roll system to further reduce the fabrication cost, which hopefully promotes the realization of practical applications.

Acknowledgements

The authors acknowledge support from the National Natural Science Foundation of China (61604090/91733301), the National Key Research and Development Program of China (2016YFA0202403), the Shaanxi Technical Innovation Guidance Project (Grant No. 2018HJCG-17), the National University Research Fund (GK261001009), the Innovative Research Team (IRT_14R33), the 111 Project (B14041), and the Chinese-National-1000-Talents-Plan program. D. Yang acknowledges the financial support from NSF I/UCRC: Center for Energy Harvesting Materials and Systems (CEHMS). S. Priya acknowledges the financial support from Air Force office of Scientific Research under award number: FA9550-17-1-0341.

Conflict of interest

The authors declare no conflict of interest.

How to cite: *Angew. Chem. Int. Ed.* **2019**, *58*, 4466–4483
Angew. Chem. **2019**, *131*, 4512–4530

- [1] I. Celik, A. B. Phillips, Z. N. Song, Y. F. Yan, R. J. Ellingson, M. J. Hebe, D. Apul, *Energy Environ. Sci.* **2017**, *10*, 1874–1884.
- [2] R. Shukla, K. Sumathy, P. Erickson, J. W. Gong, *Renewable Sustainable Energy Rev.* **2013**, *19*, 173–190.
- [3] C. Ionescu, T. Baracu, G. E. Vlad, H. Necula, A. Badea, *Renewable Sustainable Energy Rev.* **2015**, *49*, 243–253.
- [4] G. J. Hedley, A. Ruseckas, D. W. Samuel, *Chem. Rev.* **2017**, *117*, 796–837.
- [5] M. D. Kärkäs, O. Verho, E. V. Johnston, B. Åkermark, *Chem. Rev.* **2014**, *114*, 11863–12001.
- [6] J. R. Ran, J. Zhang, J. G. Yu, M. Jaroniec, S. Z. Qiao, *Chem. Soc. Rev.* **2014**, *43*, 7787–7812.
- [7] S. Sharma, K. K. Jain, A. Sharma, *Mater. Sci. Appl.* **2015**, *6*, 1145–1155.
- [8] C. Battaglia, A. Cuevas, S. D. Wolf, *Energy Environ. Sci.* **2016**, *9*, 1552–1576.
- [9] X. Liu, L. Jia, G. Fan, J. Gou, S. Liu, B. Yan, *Sol. Energy Mater. Sol. Cells* **2016**, *147*, 225–234.
- [10] X. Ren, W. Zi, Q. Ma, F. Xiao, F. Gao, S. Hu, Y. Zhou, S. Liu, *Sol. Energy Mater. Sol. Cells* **2015**, *134*, 54–59.
- [11] X. Liu, W. Zi, S. Liu, *Mater. Sci. Semicon. Proc.* **2015**, *39*, 192–199.
- [12] A. Banerjee, T. Su, D. Beglau, G. Pietka, S. Liu, Almutawalli, S. Yang, S. Guha, *IEEE J. Photovolt.* **2012**, *2*, 99–103.
- [13] A. Banerjee, S. Liu, D. Beglau, T. Su, G. Pietka, J. Yang, S. Guha, *IEEE J. Photovolt.* **2012**, *2*, 104–108.
- [14] J. D. Major, *Semicond. Sci. Technol.* **2016**, *31*, 093001.
- [15] B. M. Basol, B. M. Candless, *J. Photonics Energy* **2014**, *4*, 040996.
- [16] J. Ramanujam, U. P. Singh, *Energy Environ. Sci.* **2017**, *10*, 1306–1319.
- [17] T. Feurer, P. Reinhard, E. Avancini, B. Bissig, J. Löckinger, P. Fuchs, R. Carron, T. P. Weiss, J. Perrenoud, S. Stutterheim, S. Buecheler, A. N. Tiwari, *Prog. Photovolt: Res. Appl.* **2017**, *25*, 645–667.
- [18] D. Liang, Y. Kang, Y. Huo, Y. Chen, Y. Cui, J. S. Harris, *Nano Lett.* **2013**, *13*, 4850–4856.
- [19] W. Dang, X. Ren, W. Zi, L. Jia, S. Liu, *J. Alloys Compd.* **2015**, *650*, 1–7.
- [20] W. Zhao, D. Pan, S. Liu, *Nanoscale* **2016**, *8*, 10160–10165.
- [21] D. Wang, W. Zhao, Y. Zhang, S. Liu, *J. Energy Chem.* **2018**, *27*, 1040–1053.
- [22] A. Hagfeldt, G. Boschloo, L. C. Sun, L. Kloo, H. Pettersson, *Chem. Rev.* **2010**, *110*, 6595–6663.
- [23] G. H. Carey, A. L. Abdelhady, Z. J. Ning, S. M. Thon, O. M. Bakr, E. H. Sargent, *Chem. Rev.* **2015**, *115*, 12732–12763.
- [24] L. Y. Lu, T. Y. Zheng, Q. H. Wu, A. M. Schneider, D. L. Zhao, L. P. Yu, *Chem. Rev.* **2015**, *115*, 12666–12731.
- [25] B. Saparov, D. B. Mitzi, *Chem. Rev.* **2016**, *116*, 4558–4596.
- [26] M. M. Tavakoli, K. H. Tsui, Q. P. Zhang, J. He, Y. Yao, D. D. Li, Z. Y. Fan, *ACS Nano* **2015**, *9*, 10287–10295.
- [27] M. Ye, X. Hong, F. Zhang, X. Liu, *J. Mater. Chem. A* **2016**, *4*, 6755–6771.
- [28] F. Meillaud, M. Boccard, G. Bugnon, M. Despeisses, S. Hanni, F. J. Person, J. W. Shuttauf, M. Stükelberger, C. Ballif, *Mater. Today* **2015**, *18*, 378–384.
- [29] K. Yoo, J. Y. Kim, J. A. Lee, J. S. Kim, D. K. Lee, K. Kim, J. Y. Kim, B. S. Kim, H. Kim, W. M. Kim, J. H. Kim, M. J. Ko, *ACS Nano* **2015**, *9*, 3760–3771.
- [30] M. J. Yun, S. I. Cha, S. H. Seo, D. Y. Lee, *Sci. Rep.* **2014**, *4*, 5322.
- [31] C. R. Kagan, D. B. Mitzi, C. D. Dimitrakopoulos, *Science* **1999**, *286*, 945–947.
- [32] D. B. Mitzi, C. A. Feild, W. T. A. Harrison, A. M. Guloy, *Nature* **1994**, *369*, 467–469.
- [33] A. Kojima, K. Teshima, Y. Shirai, T. Miyasaka, *J. Am. Chem. Soc.* **2009**, *131*, 6050–6051.
- [34] G. E. Eperon, T. Leijtens, K. A. Bush, R. Prasanna, T. Green, J. T. W. Wang, D. P. McMeekin, G. Volonakis, R. L. Milot, R. May, A. Palmstrom, D. J. Slotcavage, R. A. Belisle, J. B. Patel, E. S. Parrott, R. J. Sutton, W. Ma, F. Moghadam, B. Conings, A. Babayigit, H. G. Boyen, S. Bent, F. Giustino, L. M. Herz, M. B. Johnston, M. D. McGehee, H. J. Snaith, *Science* **2016**, *354*, 861–865.
- [35] Y. Liu, Z. Yang, D. Cui, X. D. Ren, J. K. Sun, X. J. Liu, J. R. Zhang, Q. B. Wei, H. B. Fan, F. Y. Yu, X. Zhang, C. M. Zhao, S. Z. Liu, *Adv. Mater.* **2015**, *27*, 5176–5183.
- [36] a) Q. Lin, A. Armin, R. C. R. Nagiri, P. L. Burn, P. Meredith, *Nat. Photonics* **2015**, *9*, 106; b) Q. Dong, Y. Fang, Y. Shao, P. Mulligan, J. Qiu, L. Cao, J. Huang, *Science* **2015**, *347*, 967–970.
- [37] D. Shi, V. Adinolfi, R. Comin, M. Yuan, E. Alarousu, A. Buin, Y. Chen, S. Hoogland, A. Rothenberg, K. Katsiev, Y. Losovyj, X. Zhang, P. A. Dowben, O. F. Mohammed, E. H. Sargent, O. M. Bakr, *Science* **2015**, *347*, 519–522.
- [38] W. Nie, H. Tsai, R. Asadpour, J. C. Blancon, A. J. Neukirch, G. Gupta, J. J. Crochet, M. Chhowalla, S. Tretiak, M. A. Alam, H.-L. Wang, A. D. Mohite, *Science* **2015**, *347*, 522–525.
- [39] L. Dou, Y. Yang, J. You, Z. Hong, W. H. Chang, G. Li, Y. Yang, *Nat. Commun.* **2014**, *5*, 5404.
- [40] D. Yang, Z. Yang, W. Qin, Y. Zhang, S. Liu, C. Li, *J. Mater. Chem. A* **2015**, *3*, 9401–9405.
- [41] M. Liu, M. B. Johnston, H. J. Snaith, *Nature* **2013**, *501*, 395–398.
- [42] <https://www.nrel.gov/pv/assets/pdfs/pv-efficiencies-07-17-2018.pdf>.
- [43] Y. Wang, S. Bai, L. Cheng, N. Wang, J. Wang, F. Gao, W. Huang, *Adv. Mater.* **2016**, *28*, 4532–4540.
- [44] G. E. Eperon, S. D. Stranks, C. Menelaou, M. B. Johnston, L. M. Herz, H. J. Snaith, *Energy Environ. Sci.* **2014**, *7*, 982–988.
- [45] J. H. Noh, S. H. Im, J. H. Heo, T. N. Mandal, S. I. Seok, *Nano Lett.* **2013**, *13*, 1764–1768.

- [46] F. Hao, C. C. Stoumpos, R. P. H. Chang, M. G. Kanatzidis, *J. Am. Chem. Soc.* **2014**, *136*, 8094–8099.
- [47] P. Topolovsek, F. Lamberti, T. Gatti, A. Cito, J. M. Ball, E. Menna, C. Gadermaier, A. Petrozza, *J. Mater. Chem. A* **2017**, *5*, 11882–11893.
- [48] C. Wehrenfennig, G. E. Eperon, M. B. Johnston, H. J. Snaith, L. M. Herz, *Adv. Mater.* **2014**, *26*, 1584–1589.
- [49] M. H. Kumar, N. Yantara, S. Dharani, M. Graetzel, S. Mhaisalkar, P. P. Boix, N. Mathews, *Chem. Commun.* **2013**, *49*, 11089–11091.
- [50] C. Wang, L. Guan, D. Zhao, Y. Yu, C. R. Grice, Z. Song, R. A. Awni, J. Chen, J. Wang, X. Zhao, Y. Yan, *ACS Energy Lett.* **2017**, *2*, 2118–2124.
- [51] J. Feng, X. Zhu, Z. Yang, X. Zhang, J. Niu, Z. Wang, S. Zuo, S. Priya, S. Liu, D. Yang, *Adv. Mater.* **2018**, *30*, 1801418.
- [52] C. H. Chiang Bi, J. W. Lin, C. G. Wu, Y. Shao, Y. Yuan, Z. Xiao, C. Wang, Y. Gao, J. Huang, *J. Mater. Chem. A* **2016**, *4*, 13525–13533.
- [53] H. Zhou, Q. Chen, G. Li, S. Luo, T. B. Song, H. S. Duan, Z. Hong, J. You, Y. Liu, Y. Yang, *Science* **2014**, *345*, 542–546.
- [54] C. Bi, Y. Shao, Y. Yuan, Z. Xiao, C. Wang, Y. Gao, J. Huang, *J. Mater. Chem. A* **2014**, *2*, 18508–18514.
- [55] N. Pellet, P. Gao, G. Gregori, T. Y. Yang, M. K. Nazeeruddin, J. Maier, M. Grätzel, *Angew. Chem. Int. Ed.* **2014**, *53*, 3151–3157; *Angew. Chem.* **2014**, *126*, 3215–3221.
- [56] A. Dualeh, N. Tetreault, T. Moehl, P. Gao, M. K. Nazeeruddin, M. Grätzel, *Adv. Funct. Mater.* **2014**, *24*, 3250–3258.
- [57] Y. Chen, T. Chen, L. Dai, *Adv. Mater.* **2015**, *27*, 1053–1059.
- [58] C. Mombiona, O. Malinkiewicz, C. Roldan-Carmona, A. Soriano, L. Gil-Escrig, E. Bandiello, M. Scheepers, E. Edri, H. J. Bolink, *APL Mater.* **2014**, *2*, 081504.
- [59] P. Qin, S. Tanaka, S. Ito, N. Tetreault, K. Manabe, H. Nishino, M. K. Nazeeruddin, M. Grätzel, *Nat. Commun.* **2014**, *5*, 3834.
- [60] P. Cui, P. Fu, D. Wei, M. Li, D. Song, X. Yue, Y. Li, Z. Zhang, Y. Li, J. M. Mbengue, *RSC Adv.* **2015**, *5*, 75622–75629.
- [61] E. L. Unger, A. R. Bowring, C. J. Tassone, V. L. Pool, A. Gold-Parker, R. Cheacharoen, K. H. Stone, E. T. Hoke, M. F. Toney, M. D. McGehee, *Chem. Mater.* **2014**, *26*, 7158–7165.
- [62] D. Wang, H. Zhu, Z. Zhou, Z. Wang, S. Lv, S. Feng, G. Cui, *Acta Phys. Sin.* **2015**, *64*, 038403.
- [63] P. H. Huang, Y. H. Wang, J. C. Ke, C. J. Huang, *Energies* **2017**, *10*, 599.
- [64] F. Hao, C. C. Stoumpos, P. Guo, N. Zhou, T. J. Marks, R. P. H. Chang, M. G. Kanatzidis, *J. Am. Chem. Soc.* **2015**, *137*, 11445–11452.
- [65] X. Song, W. Wang, P. Sun, W. Ma, Z. Chen, *Appl. Phys. Lett.* **2015**, *106*, 033901.
- [66] K. H. Hendriks, J. J. Van Graneler, B. J. Bruijinaers, J. A. Anta, M. M. Wienk, R. A. J. Janssen, *J. Mater. Chem. A* **2017**, *5*, 2346–2354.
- [67] Y. H. Seo, E. C. Kim, S. P. Cho, S. S. Kim, S. I. Na, *Data in Brief* **2018**, *16*, 418–422.
- [68] W. Zhang, Y. Jiang, Y. Ding, M. Zheng, S. Wu, X. Lu, X. Gao, Q. Wang, G. Zhou, J. Liu, M. J. Naughton, K. Kempa, J. Gao, *Opt. Mater. Express* **2017**, *7*, 2150–2360.
- [69] P. J. Holliman, E. W. Jones, A. Connell, S. Ghosh, L. Furnell, R. J. Hobbs, *Mater. Res. Innovations* **2015**, *19*, 508–511.
- [70] N. J. Jeon, J. H. Noh, Y. C. Kim, W. S. Yang, S. Ryu, S. I. Seok, *Nat. Mater.* **2014**, *13*, 897–903.
- [71] J. Burschka, N. Pellet, S.-J. Moon, R. Humphry-Baker, P. Gao, M. K. Nazeeruddin, M. Grätzel, *Nature* **2013**, *499*, 316–319.
- [72] D. Bi, S. J. Moon, L. Haggman, G. Boschloo, L. Yang, E. M. J. Johansson, M. K. Nazeeruddin, M. Grätzel, A. Hagfeldt, *RSC Adv.* **2013**, *3*, 18762–18766.
- [73] Z. Xiao, C. Bi, Y. Shao, Q. Dong, Q. Wang, Y. Yuan, C. Wang, Y. Gao, J. Huang, *Energy Environ. Sci.* **2014**, *7*, 26192623.
- [74] W. Yongzhen, A. Islam, X. Yang, C. Qin, J. Liu, K. Zhang, W. Peng, L. Han, *Energy Environ. Sci.* **2014**, *7*, 2934–2938.
- [75] T. T. Li, Y. F. Pan, Z. Wang, Y. D. Xia, Y. H. Chen, W. Huang, *J. Mater. Chem. A* **2017**, *5*, 12602–12652.
- [76] Y. Guo, K. Shoyama, W. Sato, E. Nakamura, *Adv. Energy Mater.* **2016**, *6*, 1502317.
- [77] C. Chang, C. Chu, Y. Huang, C. Huang, S. Chang, C. Chen, C. Chao, W. Su, *ACS Appl. Mater. Interfaces* **2015**, *7*, 4955–4961.
- [78] Y. Zhao, J. Wei, H. Li, Y. Yan, W. Zhou, D. Yu, Q. Zhao, *Nat. Commun.* **2016**, *7*, 10228.
- [79] J. Mo, C. Zhang, J. Chang, H. Yang, H. Xi, D. Chen, Z. Lin, G. Lu, J. Zhang, Y. Hao, *J. Mater. Chem. A* **2017**, *5*, 13032–13038.
- [80] Y. Wang, J. Luo, R. Nie, X. Deng, *Energy Technol.* **2016**, *4*, 473–478.
- [81] N. Tripathi, Y. Shirai, M. Yanagida, A. Karen, K. Miyano, *ACS Appl. Mater. Interfaces* **2016**, *8*, 4644–4650.
- [82] J. Huang, M. Wang, L. Ding, Z. Yang, K. Zhang, *RSC Adv.* **2016**, *6*, 55720–55725.
- [83] J. H. Heo, D. H. Song, S. H. Im, *Adv. Mater.* **2014**, *26*, 8179–8183.
- [84] N. Bassiri-Gharb, Y. Bastani, A. Bernal, *Chem. Soc. Rev.* **2014**, *43*, 2125–2140.
- [85] J. H. Heo, D. H. Song, H. J. Han, S. Y. Kim, J. H. Kim, D. Kim, H. W. Shin, T. K. Ahn, C. Wolf, T. Lee, S. H. Im, *Adv. Mater.* **2015**, *27*, 3424–3430.
- [86] Y. Liang, Z. Xu, J. Xia, S. Tsai, Y. Wu, G. Li, C. Ray, L. Yu, *Adv. Mater.* **2010**, *22*, 135–138.
- [87] S. J. Lou, J. M. Szarko, T. Xu, L. Yu, T. J. Marks, L.-X. Chen, *J. Am. Chem. Soc.* **2011**, *133*, 20661–20663.
- [88] J. S. Moon, C. J. Takacs, S. Cho, R. C. Coffin, H. Kim, G. C. Bazan, A. J. Heeger, *Nano Lett.* **2010**, *10*, 4005–4008.
- [89] C. Wu, C. Chiang, Z. Tseng, M.-K. Nazeeruddin, A. Hagfeldt, M. Graetzel, *Energy Environ. Sci.* **2015**, *8*, 2725–2733.
- [90] X. Gong, M. Li, X. Shi, H. Ma, Z. Wang, L. Liao, *Adv. Funct. Mater.* **2015**, *25*, 6671–6678.
- [91] D. Liu, M. K. Gangishetty, T. L. Kelly, *J. Mater. Chem. A* **2014**, *2*, 19873–19881.
- [92] B. Conings, L. Baeten, C. De Dobbelaere, J. D’Haen, J. Manca, H. G. Boyen, *Adv. Mater.* **2014**, *26*, 20412046.
- [93] Q. Chen, H. Zhou, Z. Hong, S. Luo, H. S. Duan, H. H. Wang, Y. Liu, G. Li, Y. Yang, *J. Am. Chem. Soc.* **2014**, *136*, 622–625.
- [94] D. Yang, R. Yang, J. Zhang, Z. Yang, S. Liu, C. Li, *Energy Environ. Sci.* **2015**, *8*, 3208–3214.
- [95] H. S. Jung, N. G. Park, *Small* **2015**, *11*, 10–25.
- [96] P. P. Boix, K. Nonomura, N. Mathews, S. G. Mhaisalkar, *Mater. Today* **2014**, *17*, 16–23.
- [97] G. E. Eperon, V. M. Burlakov, A. Goriely, H. J. Snaith, *ACS Nano* **2014**, *8*, 591–598.
- [98] F. Giordano, A. Abate, J. P. C. Baena, M. Saliba, T. Matsui, S. H. Im, S. M. Zakeeruddin, M. K. Nazeeruddin, A. Hagfeldt, M. Graetzel, *Nat. Commun.* **2016**, *7*, 10379.
- [99] C. Y. Li, T. C. Wen, T. H. Lee, T. F. Guo, J. C. A. Huang, Y. C. Lin, Y. J. Hsu, *J. Mater. Chem.* **2009**, *19*, 1643–1647.
- [100] S. K. Hau, H. L. Yip, O. Acton, N. S. Baek, H. Ma, A. K.-Y. Jen, *J. Mater. Chem.* **2008**, *18*, 5113–5119.
- [101] H. Sun, J. Weickert, H. C. Hesse, L. Schmidt-Mende, *Sol. Energy Mater. Sol. Cells* **2011**, *95*, 3450–3454.
- [102] H. Lindström, A. Holmberg, E. Magnusson, S. E. Lindquist, L. Malmqvist, A. Hagfeldt, *Nano Lett.* **2001**, *1*, 97–100.
- [103] H. Lindström, A. Holmberg, E. Magnusson, L. Malmqvist, A. Hagfeldt, *J. Photochem. Photobiol. A* **2001**, *145*, 107–112.
- [104] S. A. Haque, E. Palomares, H. M. Upadhyaya, L. Otley, R. J. Potter, A. B. Holmes, J. R. Durrant, *Chem. Commun.* **2003**, *24*, 3008–3009.
- [105] F. Pichot, J. R. Pitts, B. A. Gregg, *Langmuir* **2000**, *16*, 5626–5630.

- [106] T. Kado, M. Yamaguchi, Y. Yamada, S. Hayase, *Chem. Lett.* **2003**, 32, 1056–1057.
- [107] M. Dürr, A. Schmid, M. Obermaier, S. Rosselli, A. Yasuda, G. Nelles, *Nat. Mater.* **2005**, 4, 607–611.
- [108] D. Zhang, T. Yoshida, H. Minoura, *Adv. Mater.* **2003**, 15, 814–817.
- [109] B. J. Kim, D. H. Kim, Y. Y. Lee, H. W. Shin, G. S. Han, J. S. Hong, K. Mahmood, T. K. Ahn, Y. C. Joo, K. S. Hong, N. G. Park, S. Lee, H. S. Jung, *Energy Environ. Sci.* **2015**, 8, 916–921.
- [110] D. Yang, R. Yang, X. Ren, X. Zhu, Z. Yang, C. Li, S. Liu, *Adv. Mater.* **2016**, 28, 5206–5213.
- [111] C. Roldán-Carmona, O. Malinkiewicz, A. Soriano, G. M. Espallargas, A. García, P. Reinecke, T. Kroyer, M. I. Dar, M. K. Nazeeruddin, H. J. Bolink, *Energy Environ. Sci.* **2014**, 7, 994–997.
- [112] S. S. Shin, W. S. Yang, J. H. Noh, J. H. Suk, N. J. Jeon, J. H. Park, J. S. Kim, W. M. Seong, S. I. Seok, *Nat. Commun.* **2015**, 6, 7410.
- [113] K. Wang, Y. Shi, L. Gao, R. Chi, K. Shi, B. Guo, L. Zhao, T. Ma, *Nano Energy* **2017**, 31, 424–431.
- [114] Y. Sun, J. H. Seo, C. J. Takacs, J. Seifert, A. J. Heeger, *Adv. Mater.* **2011**, 23, 1679–1683.
- [115] D. Liu, T. L. Kelly, *Nat. Photonics* **2014**, 8, 133–138.
- [116] J. H. Heo, M. H. Lee, H. J. Han, B. R. Patil, J. S. Yu, S. H. Im, *J. Mater. Chem. A* **2016**, 4, 1572–1578.
- [117] J. Feng, Z. Yang, D. Yang, X. Ren, X. Zhu, Z. Jin, W. Zi, Q. Wei, S. Liu, *Nano Energy* **2017**, 36, 1–8.
- [118] F. Qin, J. Tong, R. Ge, B. Luo, F. Jiang, T. Liu, Y. Jiang, Z. Xu, L. Mao, W. Meng, *J. Mater. Chem. A* **2016**, 4, 14017–14024.
- [119] H. Yoon, S. M. Kang, J. K. Lee, M. Choi, *Energy Environ. Sci.* **2016**, 9, 2262–2266.
- [120] Z. Zhu, J. Q. Xu, C. C. Chueh, H. Liu, Z. A. Li, X. Li, H. Chen, A. K. Y. Jen, *Adv. Mater.* **2016**, 28, 10786–10793.
- [121] M. Saliba, S. Orlandi, T. Matsui, S. Aghazada, M. Cavazzini, P. Correa-Baena, P. Gao, R. Scopelliti, E. Mosconi, K. H. Dahmen, F. D. Angelis, A. Abate, A. Hagfeldt, G. Pozzi, M. Graetzel, M. K. Nazeeruddin, *Nat. Energy* **2016**, 1, 15017.
- [122] P. Gratia, A. Magomedov, T. Malinauskas, M. Daskeviciene, A. Abate, S. Ahmad, M. Grätzel, V. Getautis, M. K. Nazeeruddin, *Angew. Chem. Int. Ed.* **2015**, 54, 11409–11413; *Angew. Chem.* **2015**, 127, 11571–11575.
- [123] P. Vivo, J. K. Salunke, A. Priimagi, *Materials* **2017**, 10, 1087.
- [124] T. M. Brown, J. S. Kim, R. H. Friend, F. Cacialli, R. Daik, W. J. Feast, *Appl. Phys. Lett.* **1999**, 75, 1679.
- [125] P. Docampo, J. M. Ball, M. Darwich, G. E. Eperon, H. J. Snaith, *Nat. Commun.* **2013**, 4, 2761.
- [126] K. Yao, X. Wang, Y. X. Xu, F. Li, *Nano Energy* **2015**, 18, 165–175.
- [127] M. Neophytou, J. Griffiths, J. Fraser, M. Kirkus, H. Chen, C. B. Nielsen, I. McCulloch, *J. Mater. Chem. C* **2017**, 5, 4940–4945.
- [128] G. Kakavelakis, T. Maksudov, D. Konios, I. Paradisanos, G. Kioseoglou, E. Stratakis, E. Kymakis, *Adv. Energy Mater.* **2017**, 7, 1602120.
- [129] J. You, Z. Hong, Q. Chen, M. Cai, T. B. Song, C. C. Chen, S. Lu, Y. Liu, H. Zhou, Y. Yang, *ACS Nano* **2014**, 8, 1674–1680.
- [130] F. Di Giacomo, A. Fakharuddin, R. Jose, T. M. Brown, *Energy Environ. Sci.* **2016**, 9, 3007–3035.
- [131] F. Hou, Z. Su, F. Jin, X. Yan, L. Wang, H. Zhao, J. Zhu, B. Chu, W. Li, *Nanoscale* **2015**, 7, 9427–9432.
- [132] J. Z. Niu, D. Yang, X. D. Ren, Z. Yang, Y. C. Liu, X. J. Zhu, W. G. Zhao, S. Z. Liu, *Org. Electron.* **2017**, 48, 165–171.
- [133] X. T. Hu, Z. Q. Huang, X. Zhou, P. W. Li, Y. Wang, Z. D. Huang, M. Su, W. J. Ren, F. Y. Li, M. Z. Li, Y. W. Chen, Y. L. Song, *Adv. Mater.* **2017**, 29, 1703236.
- [134] K.-G. Lim, S. Ahn, H. Kim, M.-R. Choi, D. H. Huh, T.-W. Lee, *Adv. Mater. Interfaces* **2016**, 3, 1500678.
- [135] K.-G. Lim, S. Ahn, Y.-H. Kim, Y. Qi, T.-W. Lee, *Energy Environ. Sci.* **2016**, 9, 932–939.
- [136] K.-G. Lim, H.-B. Kim, J. Jeong, H. Kim, J. Y. Kim, T.-W. Lee, *Adv. Mater.* **2014**, 26, 6461–6466.
- [137] H. R. Li, K. W. Fu, P. P. Boix, L. H. Wong, A. Hagfeldt, M. Grätzel, S. G. Mhaisalkar, A. C. Grimsdale, *ChemSusChem* **2014**, 7, 3420–3432.
- [138] J. Kim, J. S. Yun, X. Wen, A. M. Soufiani, C. F. J. Lau, B. Wilkinson, J. Seidel, M. A. Green, S. Huang, A. W. Y. Ho-Baillie, *J. Phys. Chem. C* **2016**, 120, 11262–11267.
- [139] S. S. Reddy, S. Shin, U. F. Aryal, R. Nishikubo, A. Saeki, M. Song, S. H. Jin, *Nano Energy* **2017**, 41, 10–17.
- [140] Q. Wang, C. Bi, J. S. Huang, *Nano Energy* **2015**, 15, 275–280.
- [141] X. T. Yin, P. Chen, M. D. Que, Y. L. Xing, W. X. Que, C. M. Niu, J. Y. Shao, *ACS Nano* **2016**, 10, 3630–3636.
- [142] H. Zhang, J. Q. Cheng, F. Lin, H. X. He, J. Mao, K. S. Wong, A. K.-Y. Jen, W. C. H. Choy, *ACS Nano* **2016**, 10, 1503–1511.
- [143] C. Bi, B. Chen, H. T. Wei, S. Deluca, J. S. Huang, *Adv. Mater.* **2017**, 29, 1605900.
- [144] K. Sakamoto, H. Kuwae, N. Kobayashi, A. Nobori, S. Shoji, J. Mizuno, *Sci. Rep.* **2018**, 8, 2825.
- [145] S. I. Na, S. S. Kim, J. Jo, D. Y. Kim, *Adv. Mater.* **2008**, 20, 4061–4067.
- [146] D. Langley, G. Giusti, C. Mayousse, C. Celle, D. Bellet, J. P. Simonato, *Nanotechnology* **2013**, 24, 452001.
- [147] M. Lee, Y. Ko, B. K. Min, Y. Jun, *ChemSusChem* **2016**, 9, 31–35.
- [148] E. Lee, J. Ahn, H.-C. Kwon, S. Ma, K. Kim, S. Yun, J. Moon, *Adv. Energy Mater.* **2018**, 8, 1702182.
- [149] J. Troughton, D. Bryant, K. Wojciechowski, M. J. Carnie, H. Snaith, D. A. Worsley, T. M. Watson, *J. Mater. Chem. A* **2015**, 3, 9141–9145.
- [150] M. Kaltenbrunner, G. Adam, E. D. Glowacki, M. Drack, R. Schwödiauer, L. Leonat, D. H. Apaydin, H. Groiss, M. C. Scharber, M. S. White, N. S. Sariciftci, S. Bauer, *Nat. Mater.* **2015**, 14, 1032.
- [151] K. Poorkazem, D. Liu, T. L. Kelly, *J. Mater. Chem. A* **2015**, 3, 9241–9248.
- [152] J. T. Wang, J. M. Ball, E. M. Barea, A. Abate, J. A. A. Webber, J. Huang, M. Saliba, I. M. Sero, J. Bisquert, H. J. Snaith, R. J. Nicholas, *Nano Lett.* **2014**, 14, 724–730.
- [153] Z. K. Liu, P. You, C. Xie, G. Q. Tang, F. Yan, *Nano Energy* **2016**, 28, 151–157.
- [154] J. Yoon, H. Sung, G. Lee, W. Cho, N. Ahn, H. S. Jung, M. Choi, *Energy Environ. Sci.* **2017**, 10, 337–345.
- [155] J. H. Heo, D. H. Shin, M. H. Jang, M. L. Lee, M. G. Kang, S. H. Im, *J. Mater. Chem. A* **2017**, 5, 21146–21152.
- [156] I. Jeon, J. Yoon, N. Ahn, M. Atwa, C. Delacou, A. Anisimov, E. I. Kauppinen, M. Choi, S. Maruyama, Y. Matsuo, *J. Phys. Chem. Lett.* **2017**, 8, 5395–5401.
- [157] X. Y. Wang, Z. Li, W. J. Xu, S. A. Kulkarni, S. K. Batabyal, S. Zhang, A. Y. Cao, L. H. Wong, *Nano Energy* **2015**, 11, 728–735.
- [158] L. B. Qiu, J. Deng, X. Lu, Z. B. Yang, H. S. Peng, *Angew. Chem. Int. Ed.* **2014**, 53, 10425–10428; *Angew. Chem.* **2014**, 126, 10593–10596.
- [159] Q. Luo, H. Ma, F. Hao, Q. Z. Hou, J. Ren, L. L. Wu, Z. B. Yao, Y. Zhou, N. Wang, K. L. Jiang, H. Lin, Z. H. Guo, *Adv. Funct. Mater.* **2017**, 27, 1703068.
- [160] Y. Li, L. Meng, Y. M. Yang, G. Xu, Z. Hong, Q. Chen, J. You, G. Li, Y. Yang, Y. Li, *Nat. Commun.* **2016**, 7, 10214.
- [161] S. T. Williams, A. Rajagopal, C.-C. Chueh, A. K.-Y. Jen, *J. Phys. Chem. Lett.* **2016**, 7, 811–819.
- [162] V. Zardetto, T. M. Brown, A. Reale, A. D. Carlo, *J. Polym. Sci. Part B* **2011**, 49, 638–648.
- [163] D. Yang, R. Yang, K. Wang, C. Wu, X. Zhu, J. Feng, X. Ren, G. Fang, S. Priya, S. Liu, *Nat. Commun.* **2018**, 9, 3239.
- [164] L. Li, S. Zhang, Z. Yang, E. E. S. Berthold, W. Chen, *J. Energy Chem.* **2018**, 27, 673–689.

- [165] Y. Yue, N. Salim, Y. Wu, X. Yang, A. Islam, W. Chen, J. Liu, E. Bi, F. Xie, M. Cai, *Adv. Mater.* **2016**, *28*, 10738–10743.
- [166] Z. Li, C. Xiao, Y. Yang, S. P. Harvey, D. H. Kim, J. A. Christians, M. Yang, P. Schulz, S. U. Nanayakkara, C. S. Jiang, *Energy Environ. Sci.* **2017**, *10*, 1234–1242.
- [167] J. I. Park, J. H. Heo, S. H. Park, K. I. Hong, H. G. Jeong, S. H. Im, H. K. Kim, *J. Power Sources* **2017**, *341*, 340–347.
- [168] B. Abdollahi Nejand, P. Nazari, S. Gharibzadeh, V. Ahmadi, A. Moshaii, *Chem. Commun.* **2017**, *53*, 747–750.
- [169] Z. Liu, A. Zhu, F. Cai, L. Tao, Y. Zhou, Z. Zhao, Q. Chen, Y.-B. Cheng, H. Zhou, *J. Mater. Chem. A* **2017**, *5*, 6597–6605.
- [170] H. Zhang, H. Wang, W. Chen, A. K.-Y. Jen, *Adv. Mater.* **2017**, *29*, 1604984.
- [171] J. Yang, B. D. Siempelkamp, D. Liu, T. L. Kelly, *ACS Nano* **2015**, *9*, 1955–1963.
- [172] Y. Fu, T. Wu, J. Wang, J. Zhai, M. J. Shearer, Y. Zhao, R. J. Hamers, E. Kan, K. Deng, X.-Y. Zhu, S. Jin, *Nano Lett.* **2017**, *17*, 4405–4414.
- [173] R. Y. F. Liu, D. A. Schiraldi, A. Hiltner, *J. Polym. Sci. Part B* **2002**, *40*, 862–877.
- [174] I. S. Kim, D. H. Cao, D. B. Buchholz, J. D. Emery, O. K. Farha, J. T. Hupp, M. G. Kanatzidis, A. B. F. Martinson, *Nano Lett.* **2016**, *16*, 7786–7790.
- [175] A. Ghosh, L. Gerenser, C. Jarman, J. Fornalik, *Appl. Phys. Lett.* **2005**, *86*, 223503.
- [176] H. C. Weerasinghe, Y. Dkhissi, A. D. Scully, R. A. Caruso, Y. B. Cheng, *Nano Energy* **2015**, *18*, 118–125.
- [177] C. Y. Chen, J. H. Chang, K. M. Chiang, H. L. Lin, S. Y. Hsiao, H. W. Lin, *Adv. Funct. Mater.* **2015**, *25*, 7064–7070.
- [178] F. Di Giacomo, V. Zardetto, G. Lucarelli, L. Cina, A. D. Carlo, M. Creatore, T. M. Brown, *Nano Energy* **2016**, *30*, 460–469.
- [179] J. Zhang, Y. Zhao, D. Yang, C. Li, S. Liu, *RSC Adv.* **2016**, *6*, 93525–93531.
- [180] W. Zi, Z. Jin, S. Liu, B. Xu, *J. Energy Chem.* **2018**, *27*, 971–989.
- [181] M. Manceau, D. Angmo, M. Jørgensen, F. C. Krebs, *Org. Electron.* **2011**, *12*, 566–574.
- [182] T. M. Brown, F. De Rossi, F. Di Giacomo, G. Mincuzzi, V. Zardetto, A. Reale, A. Di Carlo, *J. Mater. Chem. A* **2014**, *2*, 10788–10817.
- [183] J. Niu, D. Yang, Z. Yang, D. Wang, X. Zhu, X. Zhang, S. Zuo, J. Feng, S. Liu, *ACS Appl. Mater. Interfaces* **2018**, *10*, 14744–14750.
- [184] D. Yang, X. Zhou, R. Yang, Z. Yang, W. Yu, X. Wang, C. Li, S. Liu, R. Chang, *Energy Environ. Sci.* **2016**, *9*, 3071–3078.
- [185] Y.-S. Jung, K. Hwang, Y.-J. Heo, J.-E. Kim, D. Vak, D.-Y. Kim, *Adv. Opt. Mater.* **2018**, *6*, 1701182.
- [186] S. Razza, S. Castro-Hermosa, A. D. Carlo, T. M. Brown, *APL Mater.* **2016**, *4*, 091508.
- [187] K. Hwang, Y. S. Jung, Y. J. Heo, F. H. Scholes, S. E. Watkins, J. Subbiah, D. J. Jones, D. Y. Kim, D. Vak, *Adv. Mater.* **2015**, *27*, 1241–1247.
- [188] T. M. Schmidt, T. T. Larsen-Olsen, J. E. Carlé, D. Angmo, F. C. Krebs, *Adv. Energy Mater.* **2015**, *5*, 1500569.
- [189] Z. Gu, L. Zuo, T. T. Larsen-Olsen, T. Ye, G. Wu, F. C. Krebs, H. Chen, *J. Mater. Chem. A* **2015**, *3*, 24254–24260.
- [190] M. Cai, Y. Wu, H. Chen, X. Yang, Y. Qiang, L. Han, *Adv. Sci.* **2017**, *4*, 1600269.
- [191] J. E. Haysom, O. Jafarieh, H. Anis, K. Hinzer, D. Wright, *Prog. Photovolt: Res. Appl.* **2015**, *23*, 1678–1686.
- [192] K. Yang, F. Li, C. P. Veeramalai, T. Guo, *Appl. Phys. Lett.* **2017**, *110*, 083102.
- [193] Y. Li, Y. Lv, Z. Guo, L. Dong, J. Zheng, C. Chai, N. Chen, Y. Lu, C. Chen, *ACS Appl. Mater. Interfaces* **2018**, *10*, 15888–15894.
- [194] A. Swarnkar, A. R. Marshall, E. M. Sanehira, B. D. Chernomordik, D. T. Moore, J. A. Christians, T. Chakrabarti, J. M. Luther, *Science* **2016**, *354*, 92–95.
- [195] E. M. Sanehira, A. R. Marshall, J. A. Christians, S. P. Harvey, P. N. Ciesielski, L. M. Wheeler, P. Schulz, L. Y. Lin, M. C. Beard, J. M. Luther, *Sci. Adv.* **2017**, *3*, eaao4204.
- [196] M. Lee, Y. Ko, Y. Jun, *J. Mater. Chem. A* **2015**, *3*, 19310–19313.
- [197] M. Dianetti, F. Di Giacomo, G. Polino, C. Ciceroni, A. Liscio, A. D'Epifanio, S. Licocchia, T. Brown, A. Di Carlo, F. Brunetti, *Sol. Energy Mater. Sol. Cells* **2015**, *140*, 150–157.
- [198] I. Jeon, T. Chiba, C. Delacou, Y. Guo, A. Kaskela, O. Reynaud, E. I. Kauppinen, S. Maruyama, Y. Matsuo, *Nano Lett.* **2015**, *15*, 6665–6671.
- [199] M. Lee, Y. Jo, D. S. Kim, Y. Jun, *J. Mater. Chem. A* **2015**, *3*, 4129–4133.
- [200] H. Lu, J. Sun, H. Zhang, S. Lu, W. C. Choy, *Nanoscale* **2016**, *8*, 5946–5953.
- [201] L. Chen, X. Xie, Z. Liu, E. C. Lee, *J. Mater. Chem. A* **2017**, *5*, 6974–6980.
- [202] M. Lee, Y. Jo, D. S. Kim, H. Y. Jeong, Y. Jun, *J. Mater. Chem. A* **2015**, *3*, 14592–14597.
- [203] S. Pisoni, F. Fu, T. Feurer, M. Makha, B. Bissig, S. Nishiwaki, A. Tiwari, S. Buecheler, *J. Mater. Chem. A* **2017**, *5*, 13639–13647.
- [204] Y. Xiao, G. Han, H. Zhou, J. Wu, *RSC Adv.* **2016**, *6*, 2778–2784.
- [205] Y. Li, L. Meng, Y. M. Yang, G. Xu, Z. Hong, Q. Chen, J. You, G. Li, Y. Yang, Y. Li, *Nat. Commun.* **2016**, *7*, 75–81.
- [206] J. Xi, Z. Wu, B. Jiao, H. Dong, C. Ran, C. Piao, T. Lei, T. B. Song, W. Ke, T. Yokoyama, *Adv. Mater.* **2017**, *29*, 1606964.
- [207] H. Zhou, Y. Shi, K. Wang, Q. Dong, X. Bai, Y. Xing, Y. Du, T. Ma, *J. Phys. Chem. C* **2015**, *119*, 4600–4605.
- [208] Z. Yang, C. C. Chueh, F. Zuo, J. H. Kim, P. W. Liang, A. K.-Y. Jen, *Adv. Energy Mater.* **2015**, *5*, 1500328.
- [209] V. Zardetto, F. D. Giacomo, G. Lucarelli, W. Kessels, T. Brown, M. Creatore, *Sol. Energy* **2017**, *150*, 447–453.
- [210] L. Qiu, S. He, J. Yang, F. Jin, J. Deng, H. Sun, X. Cheng, G. Guan, X. Sun, H. Zhao, *J. Mater. Chem. A* **2016**, *4*, 10105–10109.
- [211] Y. Zhang, X. Hu, L. Chen, Z. Huang, Q. Fu, Y. Liu, L. Zhang, Y. Chen, *Org. Electron.* **2016**, *30*, 281–288.
- [212] M. M. Tavakoli, Q. Lin, S. F. Leung, G. C. Lui, H. Lu, L. Li, B. Xiang, Z. Fan, *Nanoscale* **2016**, *8*, 4276–4283.
- [213] L. L. Gao, L. S. Liang, X. X. Song, B. Ding, G. J. Yang, B. Fan, C. X. Li, C. J. Li, *J. Mater. Chem. A* **2016**, *4*, 3704–3710.
- [214] X. Liu, C. C. Chueh, Z. Zhu, S. B. Jo, Y. Sun, A. K.-Y. Jen, *J. Mater. Chem. A* **2016**, *4*, 15294–15301.
- [215] J. Ha, H. Kim, H. Lee, K. G. Lim, T. W. Lee, S. Yoo, *Sol. Energy Mater. Sol. Cells* **2017**, *161*, 338–346.
- [216] W. Qiu, U. W. Paetzold, R. Gehlhaar, V. Smirnov, H. G. Boyen, J. G. Tait, B. Conings, W. Zhang, C. B. Nielsen, I. McCulloch, *J. Mater. Chem. A* **2015**, *3*, 22824–22829.
- [217] Z. Chen, G. Yang, X. Zheng, H. Lei, C. Chen, J. Ma, H. Wang, G. Fang, *J. Power Sources* **2017**, *351*, 123–129.
- [218] H. G. Im, S. Jeong, J. Jin, J. Lee, D. Y. Youn, W. T. Koo, S. B. Kang, H. J. Kim, J. Jang, D. Lee, *NPG Asia Mater.* **2016**, *8*, e282.
- [219] H. Zhang, J. Cheng, D. Li, F. Lin, J. Mao, C. Liang, A. K.-Y. Jen, M. Grätzel, W. C. Choy, *Adv. Mater.* **2017**, *29*, 1604695.
- [220] J. Wei, H. Li, Y. Zhao, W. Zhou, R. Fu, H. Pan, Q. Zhao, *Chem. Commun.* **2016**, *52*, 10791–10794.
- [221] M. Park, J. Y. Kim, H. J. Son, C. H. Lee, S. S. Jang, M. J. Ko, *Nano Energy* **2016**, *26*, 208–215.
- [222] S. S. Mali, C. K. Hong, A. Inamdar, H. Im, S. E. Shim, *Nanoscale* **2017**, *9*, 3095–3104.
- [223] C. Wang, D. Zhao, Y. Yu, N. Shrestha, C. R. Grice, W. Liao, A. J. Cimaroli, J. Chen, R. J. Ellingson, X. Zhao, Y. Yan, *Nano Energy* **2017**, *35*, 223–232.

Manuscript received: August 24, 2018

Revised manuscript received: October 14, 2018

Accepted manuscript online: October 17, 2018

Version of record online: February 6, 2019